

Round Robin of High Frequency Test Methods by IPC-D24C Task Group

Glenn Oliver
Jonathan Weldon
DuPont

Research Triangle Park, NC

Chudy Nwachukwu
Isola
Chandler, AZ

John Coonrod
Rogers Corporation
Chandler, AZ

John Andresakis
Park Electrochemical
Melville, NY

David L. Wynants, Sr.
Taconic Advanced Dielectric Division
Petersburgh, NY

Abstract

Currently there is no industry standard test method for measuring dielectric properties of circuit board materials at frequencies greater than about 10 GHz. Various materials vendors and test labs take different approaches to determine these properties. It is common for these different approaches to yield varying values of key properties like permittivity and loss tangent. The D-24C Task Group of IPC has developed this round robin program to assess these various methods from the “bottom up” to determine if standardized methods can be agreed upon to provide the industry with more accurate and valid characteristics of dielectrics used in high-frequency and high-speed applications.

Problem Statement

Accurate values of relative permittivity (ϵ_r) and loss tangent ($\tan \delta$) are important characteristics for designers and fabricators in predicting electrical performance of circuits at high frequencies [1]. The most common method for evaluating these parameters at frequencies up to 10 GHz is described in IPC-TM-650-2.5.5.5 [2]. This method is equivalent to ASTM-D-3380. [3] This method excites a stripline resonator at both ends with the dielectric under test comprising most of the volume. The stripline is created by establishing intimate contact using a constant clamp force. This method is highly repeatable and is optimized for QA testing at a specific frequency. This method is not well suited for characterizing at frequencies higher than 10 GHz.

Both analog and digital applications now commonly excite dielectric materials at frequencies well above 10 GHz. Measurements at higher frequencies are especially challenging for many reasons. For instance, the wavelength of radiation at 30 GHz is < 10 mm in air and < 5 mm in FR4. This makes it more challenging to isolate the interactions of the waves with the material under test from any parasitics introduced by the test fixture. Another significant challenge at these high frequencies is that current is concentrated at the “skin” of metal surfaces. As frequencies increase, the microstructure of metal surfaces contributes more significantly to overall loss or degradation, and makes it nearly impossible to isolate the impact of the dielectric losses separate from the metal.

Introduction

In an effort to potentially determine standardized test methods at these frequencies, seven members of IPC D-24C Task Group developed a round-robin to measure ϵ_r and $\tan \delta$ for various printed circuit board (PCB) materials using different methods of their choosing and compare results.

First, this paper details the problem followed by a description of the various evaluation methods being considered; each method is described with sufficient information to allow for third party replication. Next, the results from each labs independent dielectric property characterizations are presented and subsequently compared. Finally, this paper will discuss each methods pros and cons and any conclusions or next steps.

Each test lab participant measured ten circuit board material samples up to the highest frequency for which they could provide valid data. Each participating test lab measured material from the same lot. The circuit board materials for testing were constrained to the following general properties:

- 0.5 oz Copper Clad (18 μm thick)
- Dielectric Thickness: 100-150 μm
- Relative Permittivity (ϵ_r): 2.0 – 4.0
- Loss Tangent ($\tan \delta$) ≤ 0.005

Ten materials of various constructions from multiple manufacturers were provided for characterization. Table 1 presents these materials and their general properties while assigning each material an arbitrary designator.

Table 1 –Circuit Board Materials Tested

Sample Name	Material Description	Expected Normal ϵ_r @ 10 GHz	Expected $\tan \delta$ @ 10 GHz	Nominal Thickness, mil (μm)
Sample A	Flex Polyimide	3.3	0.0040	6 (150)
Sample B	Flex Fluoropolymer / Polyimide Composite	2.5	0.0020	4 (100)
Sample C	Liquid Crystal Polymer (LCP)	3.00	0.0016	4 (100)
Sample D	Ceramic Filled Polymer on Fiberglass Substrate	3.50	0.0028	5 (125)
Sample E	Glass Microfiber Reinforced PTFE	2.20	0.0009	5 (125)
Sample F	Ceramic Filled PTFE	3.6	0.0015	5 (125)
Sample G	Micro Dispersed Ceramic in PTFE Composite on Woven Fiberglass Substrate	2.94	0.0012	5 (125)
Sample H	Ceramic filled PTFE on Woven Fiberglass Substrate	3.50	0.0020	5 (125)
Sample I	PTFE on Woven Fiberglass Substrate	2.20	0.0009	5 (125)
Sample J	Ceramic Filled Epoxy on Fiberglass Substrate	3.00	0.0011	5 (125)

The ϵ_r of each was measured using eight different methods and where it is demonstrated in this paper:

Microstrip Transmission Line Methods:

1. Extraction from impedance (ϵ_r only)
2. Group delay extraction from phase (ϵ_r only)
3. Differential phase length (ϵ_r only)

Free Space Transmission Method:

4. Free space quasi-optical (ϵ_r only)

Perturbed Resonant Cavities with Electric Field Oriented In-Plane of Dielectric:

5. Rectangular cavity and open resonator (ϵ_r and $\tan \delta$)
6. Split post dielectric resonator - SPDR (ϵ_r and $\tan \delta$)

Aperture-Coupled Stripline with Electric Field Oriented Normal to Plane of Dielectric:

7. Bereskin resonator (ϵ_r and $\tan \delta$)

Descriptions of Measurement Methods

Extraction of ϵ_r from Impedance Measurements of Microstrips

The objective of this method is to calculate normal ϵ_r values from time-domain measurements [4]. This method does not directly yield $\tan \delta$ and is a fixed value without frequency dependence. The principle of this technique is to back-calculate ϵ_r from impedance values measured on a time-domain reflectometer (TDR).

The advantage of this method is that it can utilize any microstrip transmission line or even impedance coupons on a circuit board. The disadvantages are that the values are limited by the pulse-width of the TDR and the back-calculation of ϵ_r requires a lot of assumptions.

For this study, samples were prepared by etching multiple micro strip transmission lines. These micro strip transmission lines were broken up into three line widths and two lengths. This produced six microstrip transmission lines of varying widths and lengths for each circuit board material sample. The microstrip lengths were 130 mm and 230 mm while the widths ranged from 210 μm up to 400 μm depending on the material. The three line widths were chosen for each sample based on the theoretical ϵ_r and corresponding 50 Ohm line width. The desire was for the narrow line to have impedance greater than 50 Ohms and the wide line to have impedance less than 50 Ohms with the other line falling squarely in the middle. An example of two equal line width microstrips of two different lengths can be seen in Figure 1.



Figure 1 – Two Example Microstrip Transmission Lines for Impedance Extraction

Once the microstrips were prepared, the physical dimensions of each were needed. Figure 2 shows the measurements required for the impedance extraction method. Dielectric thickness (H1) and microstrip line widths (W1) were measured using a pneumatic gauge and an optical comparator respectively. Additionally, after the impedance measurements were made, each line was cut and a cross section was taken to verify the dielectric thickness (H1), microstrip line thickness (T1), and microstrip line width on top (W2) and bottom (W1) of the microstrip. This provided the actual values needed to accurately calculate ϵ_r for the circuit board materials.

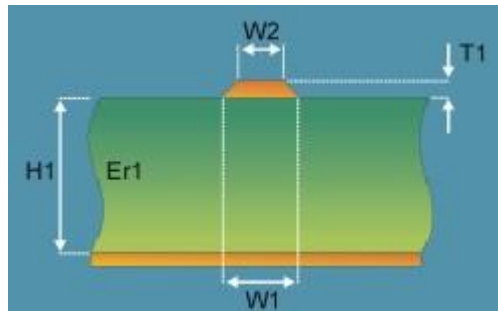


Figure 2 – Microstrip Transmission Line Cross Section [5]

Utilizing a TDR, impedances were measured for all six samples from both directions for each material. This yielded 12 impedance measurements for three line widths and two lengths. Figure 3 illustrates an example (Sample A) of the TDR impedance output versus propagation time. This figure demonstrates one of the nuances to using this impedance extraction method. The TDR provides impedance measurements versus time. Subsequently, the impedance of test cables and connectors must be considered when choosing at which point in time to measure impedance. As time directly relates to distance, a time should be chosen where the impedance being measured is somewhere within the transmission line and away from the connectors. Additionally, this point in time must be identical for all lines measured.

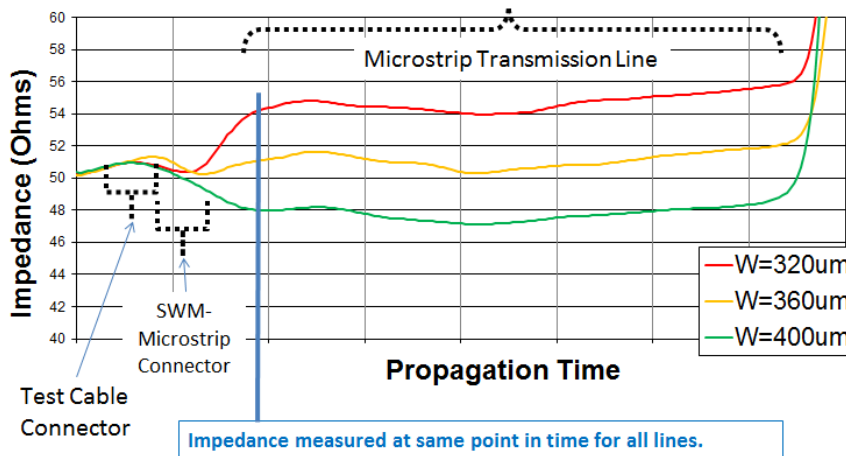


Figure 3 – Time Domain Reflectometry (TDR), Impedance versus Time

The 12 impedances for each circuit board material were measured and plotted versus measured line width. A linear regression function was developed to allow for calculation of a microstrip line with 50 Ohm characteristic impedance. This set of tests yielded impedance, dielectric thickness, microstrip line thickness, and microstrip line widths for each test sample. The measured characteristics were then used in a commercial field solver in order to back-calculate the ϵ_r . There are many calculators and field solvers available and most are suitable for this calculation.

Group Delay Extraction of ϵ_r from Phase of Microstrips

Microstrip transmission lines are a type of quasi transverse electromagnetic (TEM) structure [6]. Since the electromagnetic field propagates in media with different relative permittivity below and above the signal, the structure is inherently dispersive. The rate at which a pulse of energy traverses a transmission line is called group velocity (v_g). For dispersive transmission lines, v_g will depend on frequency. In the frequency domain, the change in phase with frequency is defined as group delay (τ_g) and can be measured and expressed as a time delay. Given the fields within the microstrip are propagating within a dielectric, the group velocity and group delay are necessary functions of the dielectric properties of the PCB on which the microstrip is constructed. Therefore, the relationship between group velocity / delay and the PCB dielectric properties allows for calculation of ϵ_r once the group delay of a particular microstrip transmission line is known.

The same microstrip lines utilized in the Impedance Extraction Method of this paper were utilized here. The only difference is that data was measured in the frequency domain instead of the time domain. The group delay method utilizes the described dispersive properties of microstrip transmission lines and the swept frequency source of a vector network analyzer (VNA) to calculate frequency dependent normal ϵ_r . Fortunately, group delay is easily measured with a VNA using the simple relationship in the following equation [7]:

$$\text{Group Delay } (\tau_g) = \frac{\Delta\varphi}{\Delta\omega} = \frac{\varphi_2 - \varphi_1}{\omega_2 - \omega_1} \quad (1)$$

where

φ = phase angle (radians)

$\omega = 2 * \pi * \text{frequency} = \text{angular frequency (Radians/Second)}$,

$\Delta\varphi$ = Difference in Phase Angle (Radians),

and

$\Delta\omega = 2\pi f = \text{Difference in Angular Frequency (Radians/Second)}$.

The phase data collected on a VNA must be unwrapped before this calculation can be fully accomplished. If the phase is not unwrapped and the difference in frequency corresponds to a 360 degree phase wrap, the calculated value will not provide a correct group delay. The wrapped and unwrapped phase can be seen in Figure 4. The group delay can be calculated locally if the phase is not unwrapped.

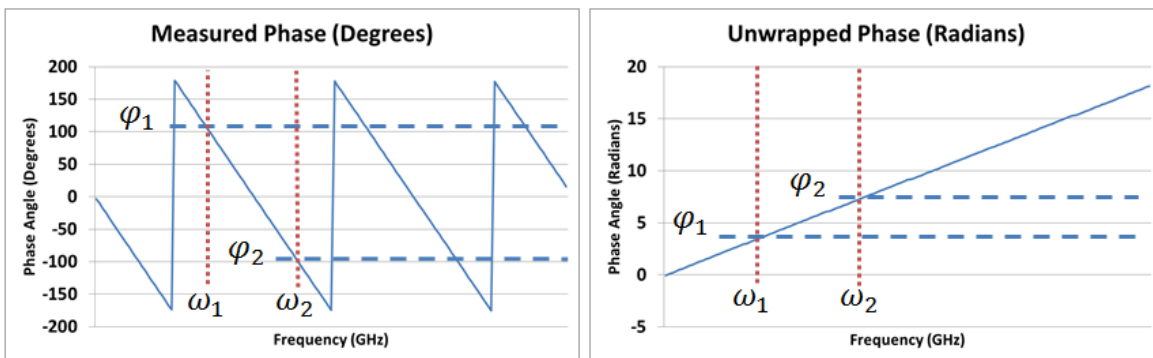


Figure 4 – Wrapped versus Unwrapped Phase for Group Delay Calculation

Once the group delay is obtained the effective dielectric constant (K_{eff}) can be calculated using the following equation:

$$\text{Effective Dielectric Constant } (K_{eff}) = \left(\frac{c * \tau_g}{L} \right)^2 \quad (2)$$

where

L = microstrip transmission line length (meters),

$$c = 3 \times 10^8 \left(\frac{\text{meters}}{\text{second}} \right),$$

and

$$\tau_g = \text{group delay (seconds)}.$$

With the effective dielectric constant (K_{eff}) of the microstrip transmission line now known, the frequency dependent ϵ_r can be calculated. The effective dielectric constant of a microstrip transmission line is not the same as the PCB material's ϵ_r . Unlike other transmission line structures, half of the microstrip is exposed to free space with ϵ_r equal to that of air while the other half is in the circuit board material. The following equation is used to calculate ϵ_r using the effective dielectric constant when

$$\frac{h}{w} < 1,$$

the closed form analytical expression follows;

$$\text{Relative Permittivity } (\epsilon_r) = \frac{1 + (2 * K_{\text{eff}} - 1) * \sqrt{1 + 12 \frac{h}{w}}}{\sqrt{1 + 12 \frac{h}{w}}} \quad (3)$$

where

$h = \text{Dielectric Thickness } (\mu\text{m}),$

and

$w = \text{Microstrip Conductor Line Width } (\mu\text{m}).$

The result is a calculated normal ϵ_r for the circuit board material at all frequencies of interest [8]. Unfortunately, this method for measuring normal permittivity does not directly yield a value for $\tan \delta$.

Microstrip Differential Phase Length ϵ_r

The microstrip differential phase length method is straight forward and (as the name implies) is the measurement of electrical phase differences for two microstrip transmission lines [9]. This method provides normal ϵ_r but does not directly provide normal $\tan \delta$. The measurement method requires only a VNA and a series of 50 Ohm microstrips of variable length.

Two lengths of microstrip were used for the measurements in this paper, one of six inches and the other of two inches; both were etched in close proximity to each other on the same panel to minimize geometric variations. Figure 5 illustrates the microstrip design and lengths used for this test.

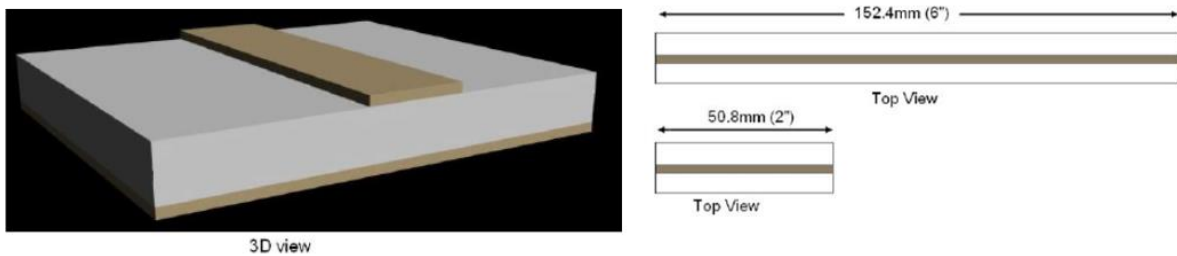


Figure 5 – Microstrip Design for Differential Phase Length Measurement

In general, one of the microstrip lines should be measured using the VNA at a specific frequency. The phase angle of the energy traveling through the microstrip should be recorded. The other microstrip of a different physical length should then be measured and the phase angle of the energy should also be recorded. Calculation of the effective dielectric constant is simple using the following equations:

$$\text{Phase Angle } (\varphi) = \omega \left(\frac{\sqrt{K_{\text{eff}}}}{c} \right) L, \quad (4)$$

$$\text{Phase Angle Difference } (\Delta\varphi) = \omega \left(\frac{\sqrt{K_{eff}}}{c} \right) \Delta L,$$

$$\text{Effective Dielectric Constant } (K_{eff}) = \left(\frac{c\Delta\varphi}{\omega\Delta L} \right)^2, \quad (5)$$

where

L = Microstrip Length (m),

and

ΔL = Difference in Microstrip Lengths (m).

Once the effective dielectric constant is calculated, ϵ_r is found by substituting the effective dielectric constant back into the equations under the group delay method, or by using a commercial transmission line calculator.

This process is iterative and should be repeated for all frequencies of interest to build a ϵ_r versus frequency curve. In this effort this process was performed up to 110 GHz. Wideband circuit measurements at millimeter wave frequencies are very difficult to obtain accurately without building multiple designs and fine tuning for the frequencies of interest. Due to the lack of fine tuning in this study, some circuits demonstrated good wideband performance while others did not.

Free Space Quasi Optical Extraction of ϵ_r

The free space quasi optical method is perhaps the most intuitive way to measure the dielectric properties of materials, as the method consists of projecting a transverse electromagnetic (TEM) wave through the material under test and recording the transmitted and reflected energy. The method is defined as quasi optical because the size of the optical components is small with regard to the wavelength and the design requires use of geometric optics [10]. Despite this more obvious configuration, it is one of the most nontrivial due to the complicated mirror assemblies, frequency dependent beam size, and the non-ideal lossy mediums that are the unclad PCB materials under test. A typical configuration is presented in Figure 6 below.

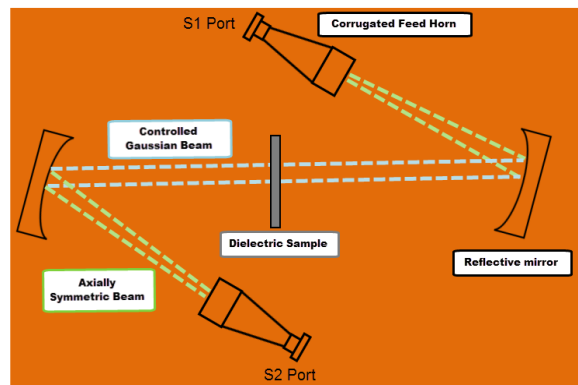


Figure 6 – Quasi Optical Measurement System

The free space quasi optical system utilizes a two port VNA connected to two corrugated feed horn antennas specifically configured for a particular frequency band (K-Band or W-Band for example). The horn antennas point toward mirrors which shape the radiated beam pattern into a Gaussian beam reflected toward the unclad dielectric material under test. The antennas and mirrors are symmetric about the circuit board material under test. These methods evaluate the change in magnitude and phase of the transmission (S21) parameters, and can yield in plane ϵ_r and $\tan \delta$ at frequencies within the band of interest. Note that any copper clad circuit board materials under test must have all copper removed before testing as this method only measures dielectric properties.

Calibrating the VNA for these measurements required the following steps:

- 1) Isolation – blocking the beam propagation path with a metal plate to account for diffraction effects at sample edges and multiple residual reflections from the antennas.
- 2) Reference – measuring the through transmission (S21) parameters without the material under test placed in the sample fixture to account for the permittivity contributions of air.
- 3) Time domain gating – Mathematical elimination of multipath signals in time domain using the sum of the distance between the horn antennas and the dielectric sample (in this case +/- 2ns).

Circuit board materials in this test were measured from 40 GHz to 60 GHz using the presented setup. The measurements and calculations were accomplished with commercially available software and the resulting data is presented in the results section. ϵ_r was determined with relative ease but the determination of loss tangent was more difficult due to the thickness of the samples tested (~5 mil).

Perturbation of Resonant Cavities to Measure ϵ_r and $\tan \delta$

The cavity resonator method is widely used as a way of characterizing dielectric properties of circuit board materials at lower frequencies. The nature of resonant methods makes them particularly useful for measuring both permittivity and $\tan \delta$ with relative ease. Collecting data and calculating ϵ_r is straight forward and requires only a suitable resonant cavity and a VNA. This method measures the in plane ϵ_r and $\tan \delta$ of a material under test by comparing the loaded (perturbed) and unloaded (unperturbed) resonant modes of a resonant cavity. The resonant frequency and quality factor will change with the loading of a resonant system with a dielectric material [8]. In order for the resonant cavity method to function, all circuit board samples must have all the copper cladding removed.

With the resonant cavity, measuring the ϵ_r and $\tan \delta$ of a material is a quick and repeatable process. First, the resonant cavity must be connected to the VNA and the resonant frequencies and quality factors within the frequency band of interest must be mapped. Once this is accomplished the circuit material under test must be placed in the resonator and the resonant frequencies and quality factors must be mapped again.

Two different cavity resonant methods were implemented. The first was a rectangular waveguide cavity resonator, shown in Figure 7, which was used to characterize the dielectric properties of the circuit board materials up to 10 GHz.



Figure 7 – Rectangular Cavity Resonator

Specifically, the waveguide resonator is setup with only enough space to fit the circuit board material sample between the two halves of the resonant cavity. This is done to allow for the material under test to be inserted and removed without disturbing the cavity dimensions. The cavity is designed to have six resonant modes at frequencies of approximately 2.2 GHz, 3.4 GHz, 5.0 GHz, 6.8 GHz, 8.6 GHz and 10.4 GHz. Data collection and processing is done through automated commercial software that interfaces directly with the VNA. It's important to note that the process was done twice for each sample, one with the sample in a vertical orientation and the other with the sample rotated 90 degrees in a horizontal orientation. This was done to determine if there are any differences in the in-plane permittivity and $\tan \delta$ based on material orientation. The rectangular cavity has the advantage of being very simple and quick, but the precision of $\tan \delta$ is limited to about 0.0005-0.001 since the resonator Q ranges between 2000-7000.

The second resonator was an open cavity, shown in Figure 8, which implements two concave spherical reflectors to create a concentric resonant cavity. This cavity was used to characterize the circuit board materials up to 40 GHz. The resonant mode frequencies are determined by the distance between the reflectors. Choosing the optimum cavity spacing requires some experimentation to minimize interfering modes across the range of thickness and permittivity in the materials being measured. A configuration was chosen such that five resonances could be consistently and repeatedly measured. 26 GHz, 40 GHz, 49 GHz, 56 GHz, and 60 GHz were chosen. Data collection and processing is done through commercial software that interfaces directly with the VNA. In both cavities, the sample is placed in the middle and evaluated in both the vertical and horizontal orientation. The open resonator is capable of precision for $\tan \delta$ measurement of about 0.0001 since the Q of the resonator is 50,000 – 100,000. The disadvantage of this technique is that it is quite tedious to perform and repeatability is limited by mechanical and ambient environmental stability that needs to be maintained for the fixture.

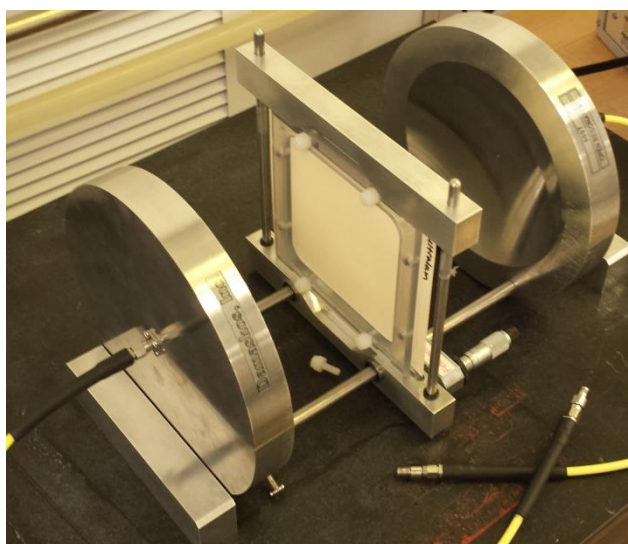


Figure 8 – Open Resonator

Figure 9 illustrates the overall resonant method concept. The higher quality factor (Q_c) waveform is of the resonant cavity absent a circuit board material sample and the lower quality factor (Q_s) waveform is of the same resonant cavity with a material under test present. The resonant frequency (f_c) of the empty cavity is clearly shifted to a lower frequency (f_s) and the quality factor (Q_s) is clearly lower with a sample present. The resonant frequencies and bandwidths of the unloaded cavity and the loaded cavity should be measured and quality factor calculated for the frequencies of interest [12].

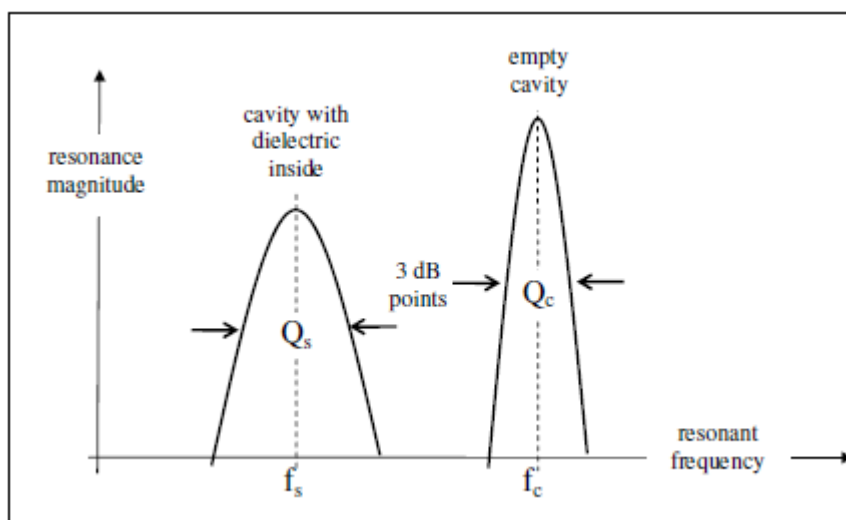


Figure 9 – Illustration of Resonant Cavity Method

Once mapped, the equations below can be used to calculate ϵ_r and $\tan \delta$. These equations compare the differences in the resonant frequency and quality factor from the unloaded cavity to the cavity with a circuit board material present.

$$\text{Relative Permittivity } (\epsilon_r) = \frac{\epsilon}{\epsilon_0} = \epsilon_r' - j\epsilon_r'' \quad (6)$$

$$\text{Loss Tangent } (\tan \delta) = \left(\frac{\epsilon_r''}{\epsilon_r'} \right) = \frac{1}{Q} \quad (7)$$

where

$$\text{Real Relative Permittivity } (\epsilon_r') = \frac{V_c(f_c - f_s)}{2V_s f_s} V_c + 1, \quad (8)$$

$$\text{Imaginary Relative Permittivity } (\epsilon_r'') = \frac{V_c}{4V_s} \left(\frac{1}{Q_s} - \frac{1}{Q_c} \right), \quad (9)$$

$$\text{Quality Factor of Unloaded Cavity } (Q_c) = \frac{f_c}{\Delta f} \quad (10)$$

$$\text{Quality Factor of Cavity with Sample } (Q_s) = \frac{f_s}{\Delta f}, \quad (11)$$

V_c = Volume of Cavity,

V_s = Volume of Sample,

f_c = resonant frequency of unloaded the cavity (Hz),

f_s = resonant frequency of the cavity with sampe (Hz),

and

$$\Delta f = f_{\text{upper half power cutoff (3 dB)}} - f_{\text{lower half power cutoff (3 dB)}}.$$

Split Post Dielectric Resonator (SPDR) to Measure ϵ_r and $\tan \delta$

The split post dielectric resonator, as seen in Figure 11, utilizes two circular dielectric resonators to measure ϵ_r and $\tan \delta$ on a circuit board material. The method functions similarly to the previously described resonant cavities in that the unloaded quality factor (Q_c) and resonant frequency (f_c) of the resonator without a material sample is compared to the loaded cavities change in resonance quality factor (Q_s) and shifted frequency (f_s) with a material sample present. However, this method is different in that the Rayleigh-Ritz method is used to compute the resonant frequencies, the unloaded quality factors and all other parameters of the SPDR [13]. In this study, all calculations and measurements were accomplished with commercially available software and hardware.

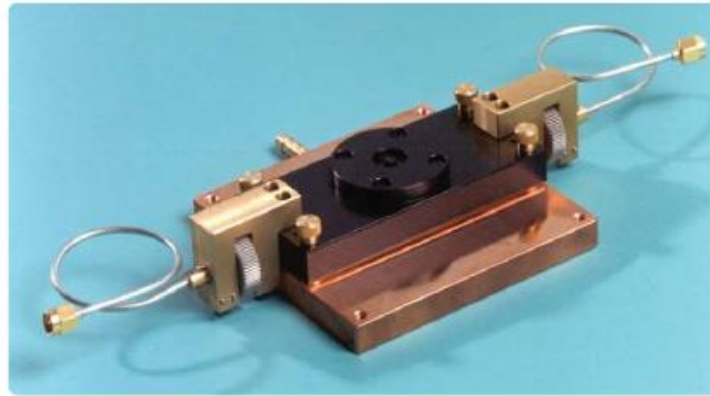


Figure 11 – Split Post Dielectric Resonator

Figure 12 displays the cross section of the SPDR system. The two dielectric resonators are seen on top and bottom with the feed loops at the left and right. The cavity is setup such that the dielectric does not fill the entire cavity requiring that the air gap height (h_G) is greater than the sample height (h). The cavities unloaded resonant frequencies and quality factors are measured with an air gap of height h_G , and the shifted resonant frequencies and quality factors are measured with the sample inserted within the fixture without adjusting this overall height.

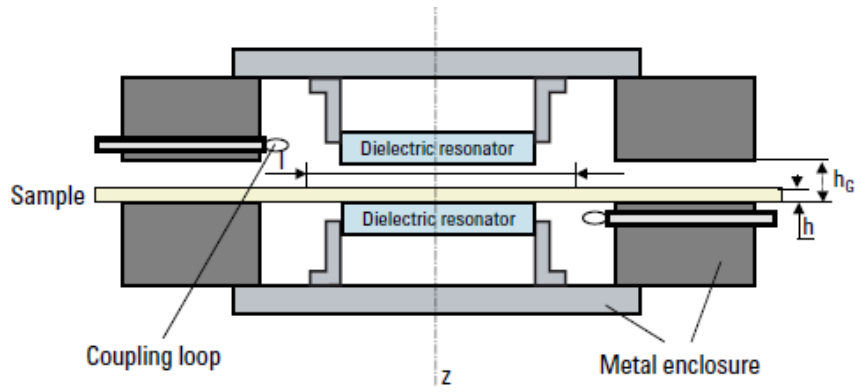


Figure 12 – Split Post Dielectric Resonator Cross Section

As with other resonant methods, the dielectric characteristics can only be measured at certain fixed frequencies and the sample material must have all copper removed before testing. Additionally, the values of ϵ_r and $\tan \delta$ are in plane with the material and not orthogonal. SPDR measurements were taken on all 10 samples at resonant frequencies of 10 GHz and 20 GHz.

Bereskin Clamped Embedded Stripline Resonator to Measure ϵ_r and $\tan \delta$

The Bereskin clamped imbedded stripline resonator test method operates from approximately 1 GHz up to 22 GHz. This resonant method, with a setup shown in Figure 13, operates through the use of aperture launched and received energy that excites the resonant modes in a copper strip clamped between two sheets of dielectric material under test. This method is similar to IPC-TM-650-2.5.5.5.1, Stripline Test for Complex Relative Permittivity of Circuit Board Materials to 14 GHz [14], but is more thoroughly explained in Dr. Bereskin’s two patents[15][16]. This method has several pros, insomuch as it measures normal permittivity and $\tan \delta$ directly. However, a downside is that air entrapped between the two dielectric layers creates measurement error due to localized variations in dielectric properties. The copper is removed from the dielectric prior to testing and the same copper strip is used in all the tests. The copper strip is stand-alone instead of being defined by etching in alternate stripline resonant methods. The specific test bed utilizes a signal generator and power meters, but a VNA can also be used if desired.

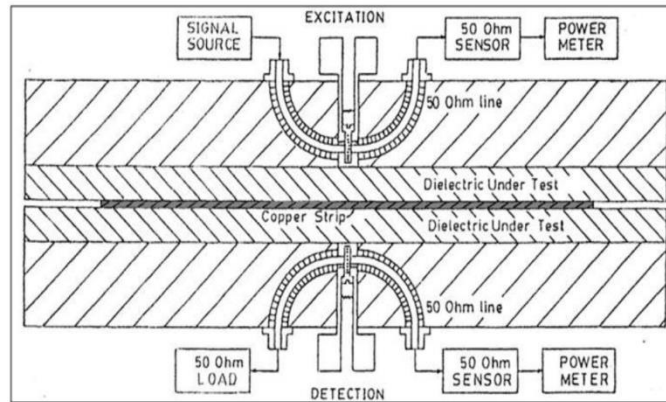


Figure 13 – Clamped Embedded Stripline Resonator

The output power from the resonator is received at the power meter connected opposite the signal source. Sweeping the signal source through all frequencies in the band and comparing variation in amplitude over frequency yields the resonant frequencies (f_s) and quality factors (Q_s) of the system. Unlike the other resonators the clamped embedded stripline resonator does not work as a simple function of resonant frequency shifts from an unloaded to a loaded cavity. The resonator is a copper stripline and only functions with the material under test placed in the fixture therefore has no free space baseline for relative comparison. The basic calculations for ϵ_r and $\tan \delta$ are shown in the following equations:

$$\text{Relative Permittivity } (\epsilon_r) = \left(\frac{c}{2.54 f_s (L + \Delta L)} \right)^2 \tag{12}$$

where

$$c = 3 \times 10^8 \left(\frac{\text{meters}}{\text{second}} \right)$$

f_s = resonant frequencies L = physical length of resonator copper strip (meters)

ΔL = effective increase in resonator length from fringing field (meters);

and

$$\text{Loss Tangent } (\tan \delta) = \frac{1}{Q_s} - \frac{1}{Q_c}, \quad (13)$$

where

Q_s = Quality Factor of the Cavity with Sample

and

Q_c = Quality Factor of the Unloaded Cavity.

The quality factor of the cavity with sample (Q_s) is easily calculated using the above equations and the measured resonator values. However, the quality factor of the unloaded cavity (Q_c) is not so readily determined. The analytical approach is detailed in IPC-TM-650-2.5.5.5.1 as is the method for calculating the effective increase in resonator length from fringing field.

This study considered nine, and in some instances 10, resonant frequencies in the 1 GHz to 22 GHz band. The measured values of ϵ_r and $\tan \delta$ were obtained for each sample and were averaged for comparison. The dielectric under test is presumed to be a single block on either side of the copper strip. Generally 60 mils [1.524mm] is preferred as in IPC-TM-650 2.5.5.5. In this case, 5 mil [.127mm] material was supplied and stacked so the resulting ϵ_r values are skewed lower due to entrapped air from inconsistent thicknesses and embedded copper surface roughness pockets associated with cladding removal.

Results

Extraction of ϵ_r from Impedance Measurements of Microstrips

As mentioned previously, each circuit board material sample was broken up into six microstrip transmission lines of varying lengths and line widths. Each line was measured with the TDR from both ends of the microstrip. The distance into the strip line was identical for each measurement. Figure 14 shows the 12 impedances measured for each sample along with the linear regression. Additionally, each materials microstrip line width for 50 Ohm characteristic impedance is noted along with the measured dielectric thickness.

Figure 14 – TDR Microstrip Transmission Line Impedances

Once the characteristic impedance and board parameters were measured, the values were entered manually into the field solver software and the ϵ_r was calculated. Table 2 shows the calculated normal ϵ_r for all 10 material samples. Again, this value for ϵ_r does not take into account frequency dependence.

Table 2 – Relative Permittivity via Impedance Extraction Method

Sample Name	Calculated Normal Relative Permittivity (ϵ_r)	Sample Name	Calculated Normal Relative Permittivity (ϵ_r)
Sample A	2.97	Sample F	3.42
Sample B	2.10	Sample G	2.20
Sample C	2.87	Sample H	3.08
Sample D	3.03	Sample I	1.84
Sample E	1.82	Sample J	2.69

Group Delay Extraction of ϵ_r from Phase of Microstrips

Figure 15 displays the smoothed effective dielectric constant (K_{eff}) versus frequency for each sample with the characteristic impedance closest to 50 Ohms. The corresponding physical parameters of each line are also noted. A moving average filter was used in order to smooth the effective dielectric constant and remove any abnormalities. Note the average effective dielectric constant is not the same as ϵ_r .

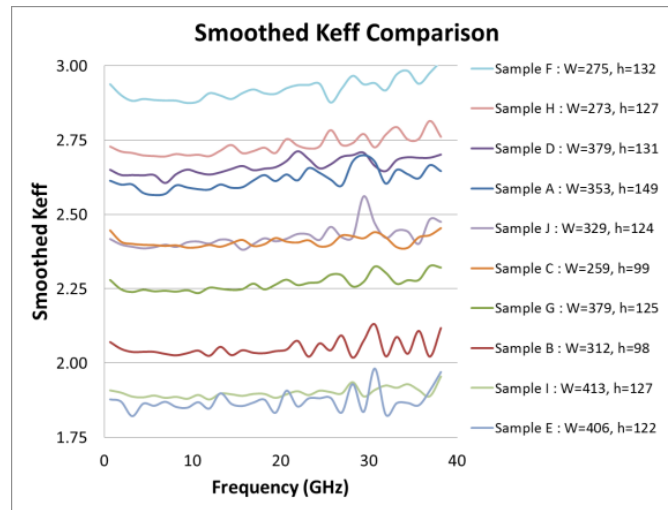


Figure 15 – Smoothed Effective Dielectric Constant from Group Delay

Figure 16 presents a comparison of each samples calculated ϵ_r . The line widths and dielectric thicknesses of each sample presented are also presented.

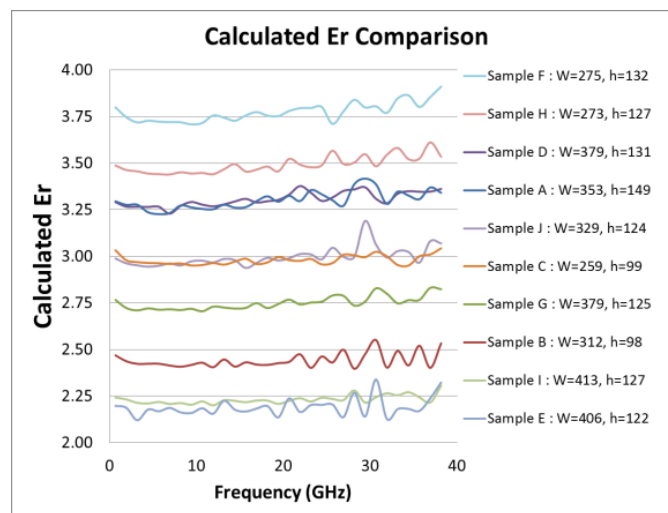


Figure 16 – Averaged Effective Dielectric Constant and Calculated Relative Permittivity Comparison

Microstrip Differential Phase Length ϵ_r

Figure 17 shows ϵ_r as calculated from the microstrip differential phase length method. Measurements were made from 1 GHz to 110 GHz.

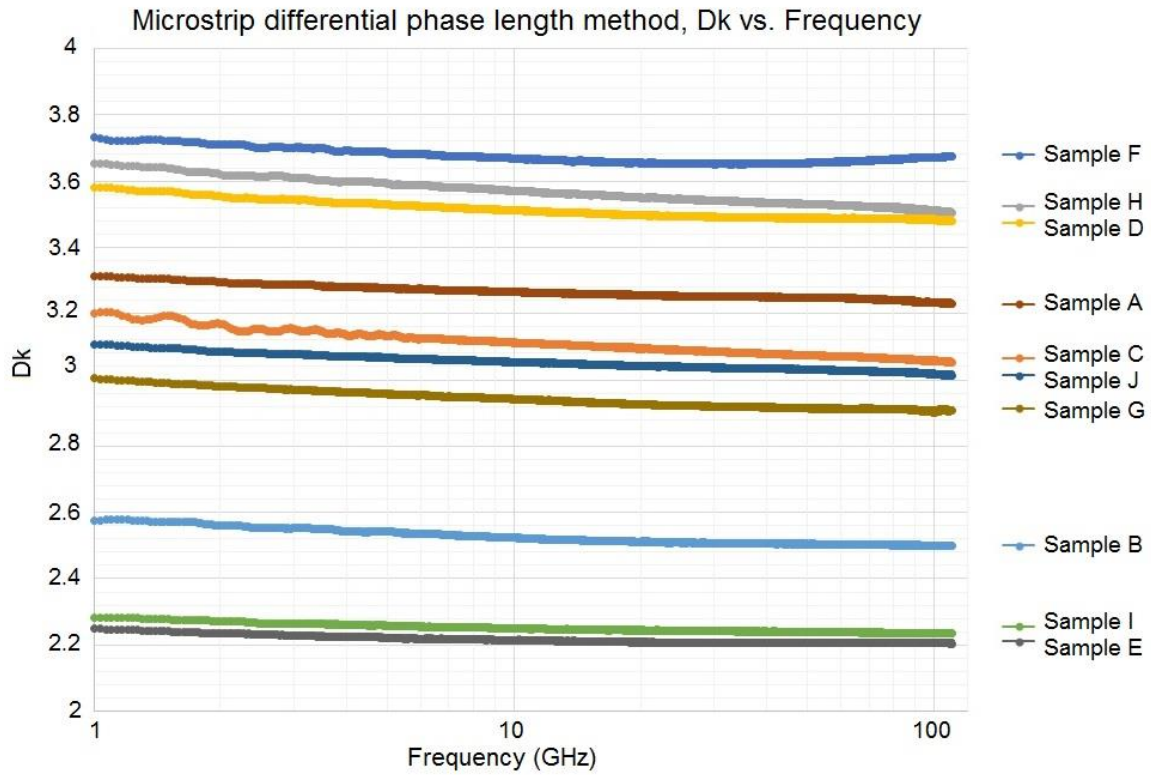


Figure 17 – Relative Permittivity from Microstrip Differential Phase Length Method

Free Space Quasi Optical Extraction of ϵ_r

Figures 18 through 27 present plots of ϵ_r for all materials as captured by the free space quasi optical method. The ϵ_r is shown from 35 GHz to 65 GHz, but is only valid from 40 GHz to 60 GHz. The elongated elliptical window shown over the real dielectric permittivity (red trace) on each plot is the gated window for each sample. This window is also seen in the Cole-Cole plot as indicated with the two black vertical dotted lines along the horizontal axis (Real Permittivity).

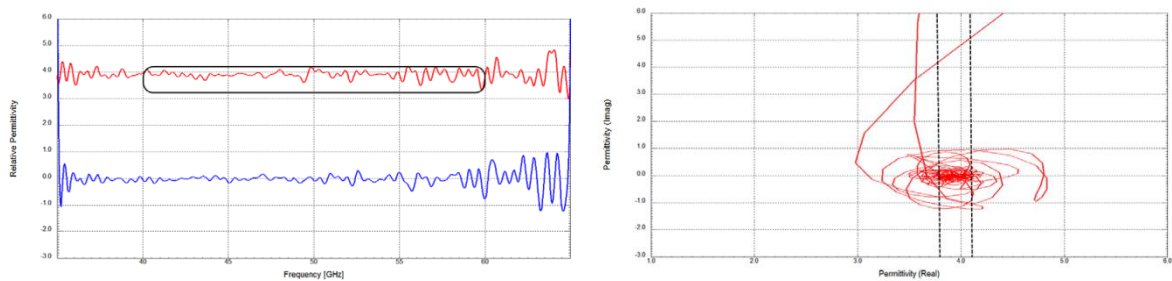


Figure 18 – Sample A - Relative Permittivity and Cole-Cole Plot

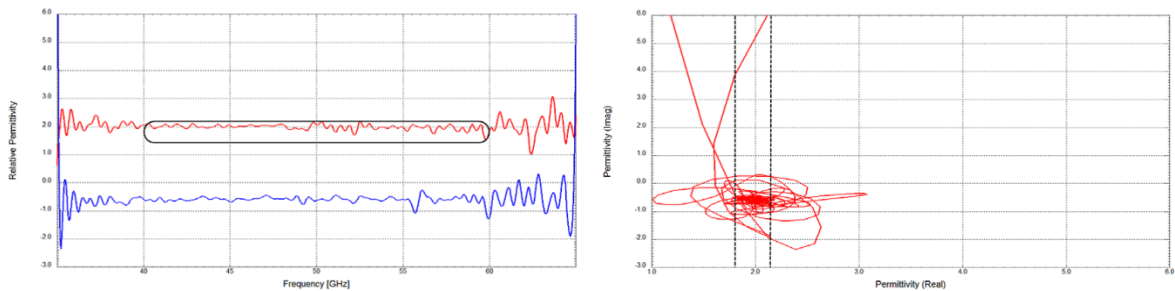


Figure 19 – Sample B - Relative Permittivity and Cole-Cole Plot

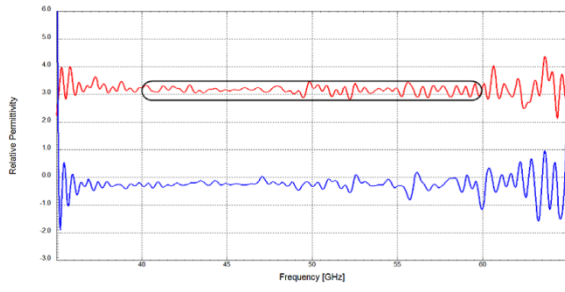


Figure 20 – Sample C - Relative Permittivity and Cole-Cole Plot

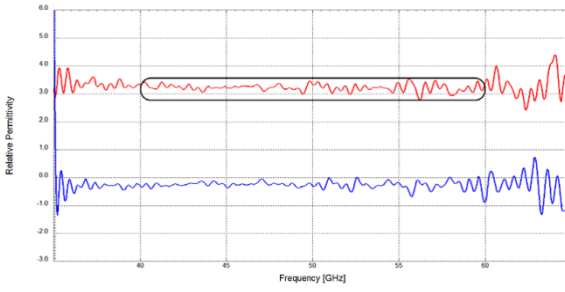
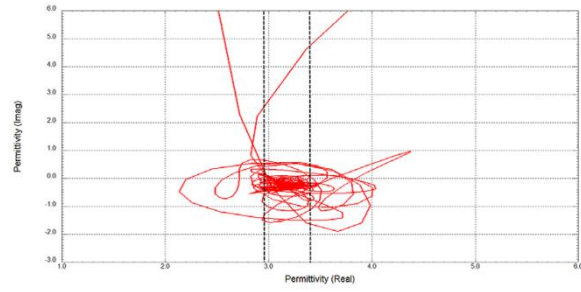


Figure 21 – Sample D - Relative Permittivity and Cole-Cole Plot

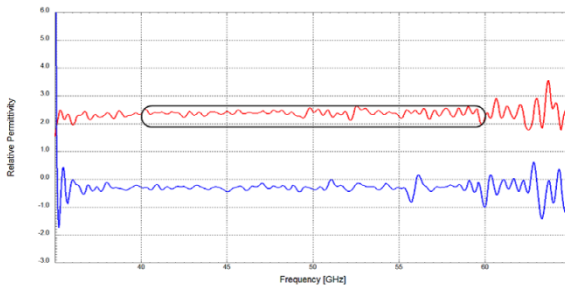
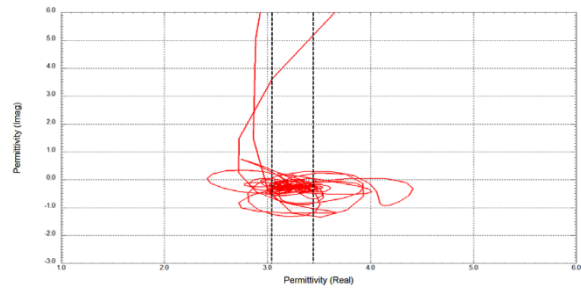


Figure 22 – Sample E - Relative Permittivity and Cole-Cole Plot

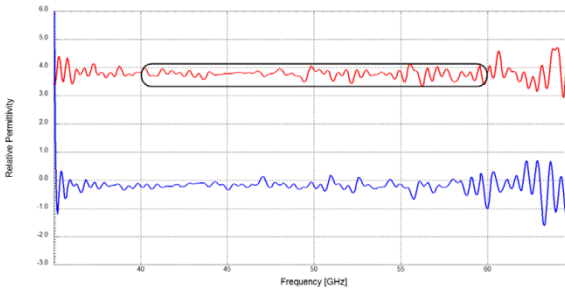
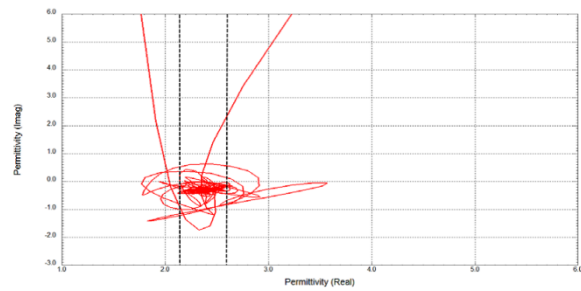


Figure 23 – Sample F - Relative Permittivity and Cole-Cole Plot

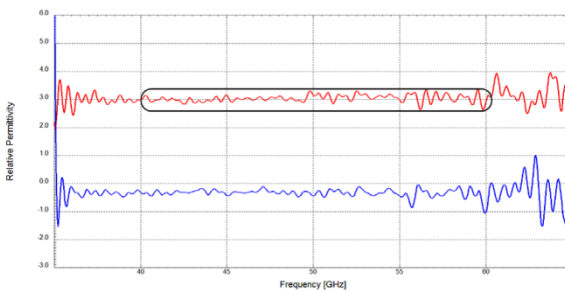
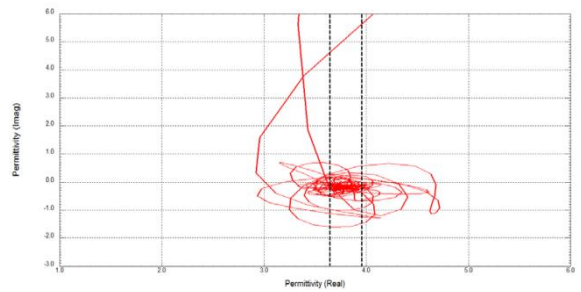
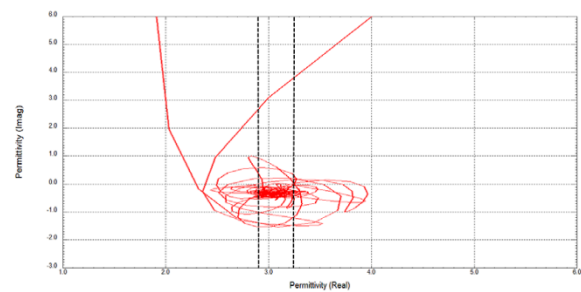


Figure 24 – Sample G - Relative Permittivity and Cole-Cole Plot



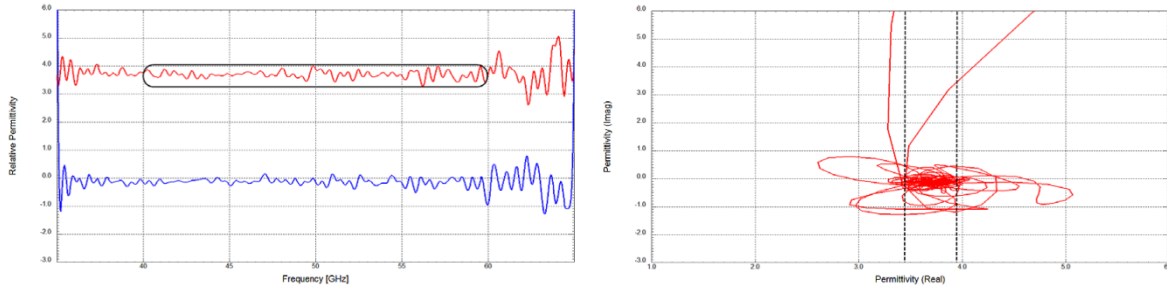


Figure 25 – Sample H – Relative Permittivity and Cole-Cole Plot

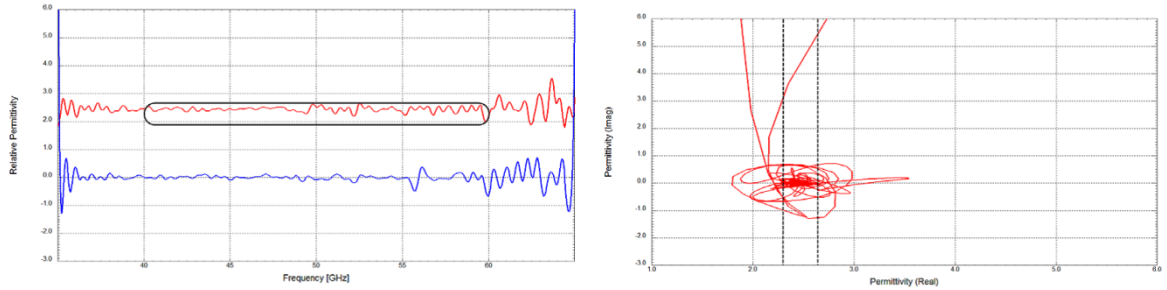


Figure 26 – Sample I - Relative Permittivity and Cole-Cole Plot

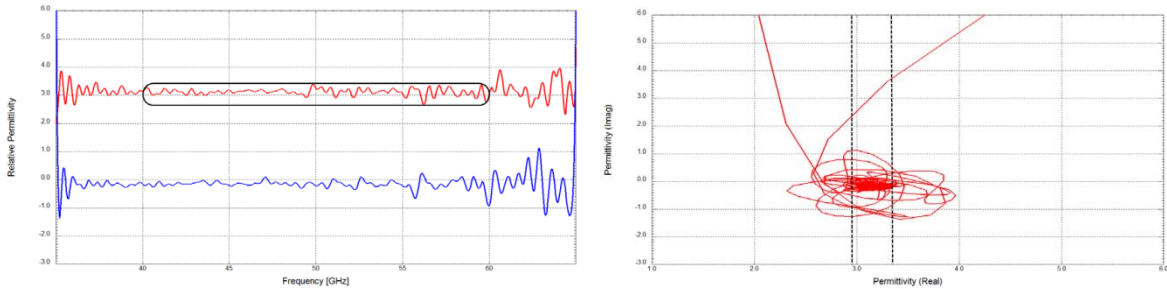


Figure 27 – Sample J - Relative Permittivity and Cole-Cole Plot

The values for each sample were averaged within the window from 40 GHz to 60 GHz. Table 3 presents these averages.

Table 3 – Relative Permittivity from Free Space Quasi Optical Method

Sample Name	In-Plane Relative Permittivity (ϵ_r)	Sample Name	In-Plane Relative Permittivity (ϵ_r)
Sample A	3.9	Sample F	3.8
Sample B	2.0	Sample G	3.1
Sample C	3.2	Sample H	3.7
Sample D	3.25	Sample I	2.5
Sample E	2.35	Sample J	3.15

Perturbation of Resonator Cavities to Measure ϵ_r and $\tan \delta$

The results from both the rectangular waveguide resonator and free space resonant cavity were combined into one plot in Figure 28. The two methods do not show any obvious discontinuities and the values for ϵ_r and $\tan \delta$ are stable and without significant variation. In the summary plot, values below 20 GHz were measured with the closed rectangular cavity while values above 20 GHz were measured with the open resonator.

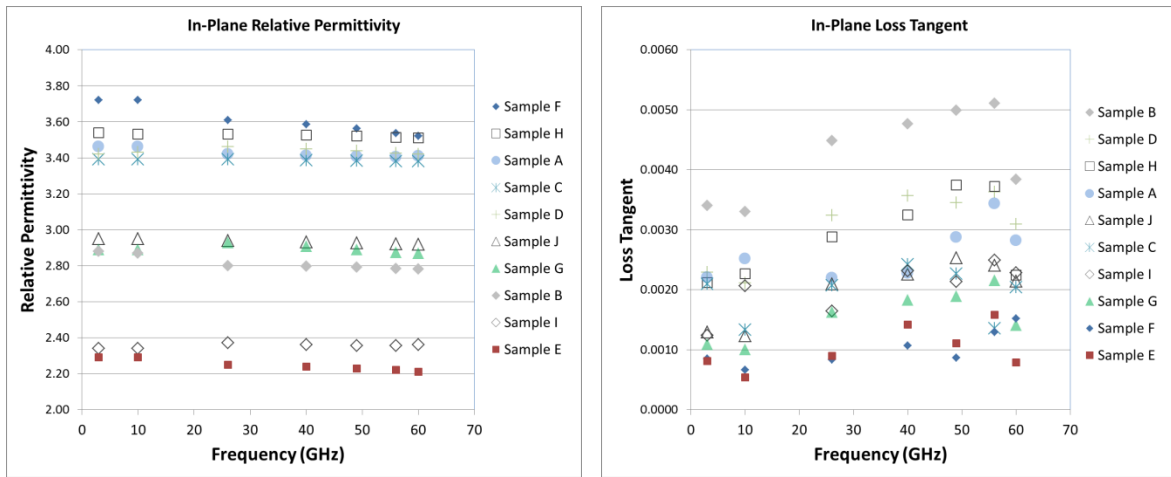


Figure 28 – Resonant Cavity Method In-Plane Relative Permittivity and Loss Tangent

The plots are broken out in tables of ϵ_r in Table 4 and $\tan \delta$ in Table 5.

Table 4 – Relative Permittivity from Perturbed Resonators

Frequency (GHz) \ Sample Name	3 (GHz) Rect.	10 (GHz) Rect.	26 (GHz) Open	40 (GHz) Open	49 (GHz) Open	56 (GHz) Open	60 (GHz) Open	Average
Sample A	3.46	3.46	3.42	3.41	3.41	3.40	3.41	3.42
Sample B	2.88	2.87	2.80	2.80	2.79	2.78	2.78	2.81
Sample C	3.39	3.39	3.39	3.39	3.38	3.38	3.38	3.39
Sample D	3.42	3.43	3.46	3.45	3.44	3.42	3.42	3.43
Sample E	2.29	2.29	2.25	2.24	2.23	2.22	2.21	2.25
Sample F	3.72	3.72	3.61	3.59	3.56	3.54	3.52	3.61
Sample G	2.89	2.89	2.93	2.91	2.89	2.88	2.87	2.89
Sample H	3.54	3.53	3.53	3.53	3.52	3.51	3.51	3.52
Sample I	2.34	2.34	2.37	2.36	2.36	2.36	2.36	2.35
Sample J	2.95	2.95	2.94	2.93	2.93	2.92	2.92	2.93

Table 5 – Loss Tangent from Perturbed Resonator Method

Frequency (GHz) \ Sample Name	3 (GHz) Rect.	10 (GHz) Rect.	26 (GHz) Open	40 (GHz) Open	49 (GHz) Open	56 (GHz) Open	60 (GHz) Open
Sample A	0.0022	0.0025	0.0022	0.0023	0.0029	0.0034	0.0028
Sample B	0.0034	0.0033	0.0045	0.0048	0.0050	0.0051	0.0038
Sample C	0.0021	0.0013	0.0021	0.0024	0.0023	0.0014	0.0020
Sample D	0.0023	0.0021	0.0032	0.0036	0.0035	0.0036	0.0031
Sample E	0.0008	0.0005	0.0009	0.0014	0.0011	0.0016	0.0008
Sample F	0.0008	0.0007	0.0008	0.0011	0.0009	0.0013	0.0015
Sample G	0.0011	0.0010	0.0016	0.0018	0.0019	0.0022	0.0014
Sample H	0.0021	0.0023	0.0029	0.0032	0.0037	0.0037	0.0022
Sample I	0.0012	0.0021	0.0016	0.0023	0.0021	0.0025	0.0023
Sample J	0.0013	0.0012	0.0021	0.0023	0.0025	0.0024	0.0021

Split Post Dielectric Resonator (SPDR) to Measure ϵ_r and $\tan \delta$

Table 6 presents the results from the SPDR method. Only two resonant frequencies were used in this collection.

Table 6 – Relative Permittivity and Loss Tangent from Split Post Dielectric Resonator (SPDR) Method

Sample Designator	10 GHz		20 GHz	
	ϵ_r	$\tan \delta$	ϵ_r	$\tan \delta$
Sample A	3.448	0.0017	3.440	0.0027
Sample B	2.789	0.0016	2.787	0.0020
Sample C	3.317	0.0018	3.308	0.0025
Sample D	3.445	0.0025	3.436	0.0041
Sample E	2.260	0.0007	2.254	0.0015
Sample F	3.577	0.0008	3.568	0.0020
Sample G	2.991	0.0011	2.893	0.0024
Sample H	3.424	0.0023	3.402	0.0038
Sample I	2.297	0.0014	2.281	0.0019
Sample J	2.894	0.0017	2.883	0.0024

Bereskin Clamped Embedded Stripline Resonator to Measure ϵ_r and $\tan \delta$

The Bereskin clamped embedded stripline resonator method results are presented in Figure 29. The measured ϵ_r shows good stability and linearity over the band. The measured $\tan \delta$ is a bit noisy for some samples.

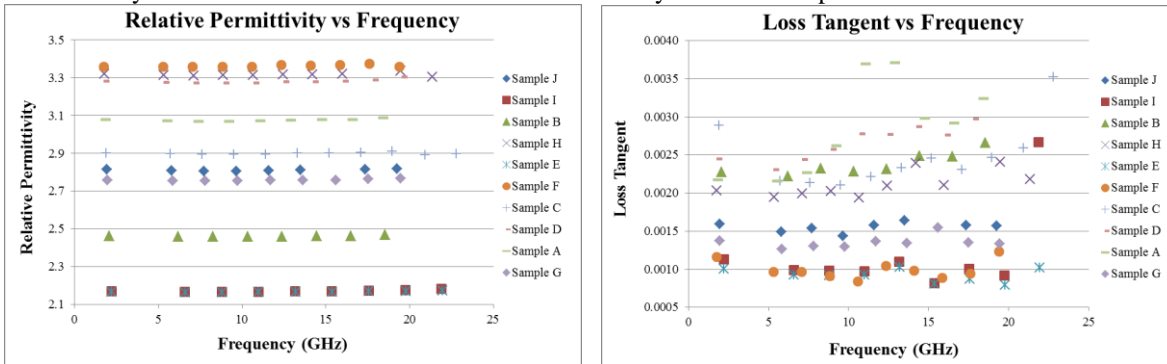


Figure 29 – Relative Permittivity and Loss Tangent from Bereskin Clamped Embedded Stripline Resonator Method

Table 7 shows the average ϵ_r and $\tan \delta$ values measured for every sample over the entire band.

Table 7 – Relative Permittivity and Loss Tangent from Bereskin Clamped Embedded Stripline Resonator Method

Sample Name	ϵ_r	$\tan \delta$	Frequency Range (GHz)
Sample A	3.08	.0029	1.84 – 18.42
Sample B	2.46	.0024	2.06 – 18.54
Sample C	2.9	.0024	1.90 – 22.81
Sample D	3.28	.0027	1.79 – 19.58
Sample E	2.17	.0009	2.20 – 21.96
Sample F	3.36	.0010	1.76 – 19.40
Sample G	2.76	.0014	1.95 – 19.45
Sample H	3.32	.0021	1.77 – 21.35
Sample I	2.17	.0010	2.20 – 21.89
Sample J	2.81	.0016	1.93 – 19.26

Comparison

The seven methods yielded somewhat different results. The data was first averaged and compared for each method over each respective frequency band. This gives a relative idea of how the various methods performed versus one another with regards to their overall agreement on a materials ϵ_r . Table 8 presents the average ϵ_r as measured by each method.

Table 8 – Averaged Relative Permittivity Comparison for All Methods

Sample Name	Impedance Extraction	Group Delay	Differential Phase Length	Quasi Optical	Perturbed Resonators	SPDR	Bereskin Stripline
Sample A	2.97	3.30	3.27	3.9	3.42	3.444	3.08
Sample B	2.10	2.44	2.55	2.0	2.81	2.788	2.46
Sample C	2.87	2.98	3.13	3.2	3.39	3.313	2.9
Sample D	3.03	3.31	3.53	3.25	3.43	3.441	3.28
Sample E	1.82	2.19	2.23	2.35	2.25	2.257	2.17
Sample F	3.42	3.77	3.63	3.8	3.61	3.573	3.36
Sample G	2.20	2.75	2.96	3.1	2.89	2.942	2.76
Sample H	3.08	3.49	3.58	3.7	3.52	3.413	3.32
Sample I	1.84	2.23	2.27	2.5	2.35	2.289	2.17
Sample J	2.69	3.00	3.06	3.15	2.93	2.889	2.81

Once the methods were compared against one another, the averages were weighed against the designed ϵ_r . Table 9 shows the percentage difference in the measured average ϵ_r versus the expected value per the nominal values in data sheets. The bottom row shows the average percentage difference.

Table 9 – Percent Difference of Measured Average vs Data Sheet Normal Relative Permittivity

Sample Name	Impedance Extraction	Group Delay	Differential Phase Length	Quasi Optical	Perturbed Resonators	SPDR	Bereskin Stripline
Sample A	10	0.0	0.9	18	3.6	1.6	6.7
Sample B	16	2.4	2.0	20	12	12	1.6
Sample C	4.3	0.7	4.3	7.0	13	10	3.3
Sample D	25	5.4	0.9	7.1	2.0	1.2	6.3
Sample E	17	0.5	1.4	6.8	2.3	2.6	1.4
Sample F	5.0	4.7	0.8	5.6	0.3	0.8	6.7
Sample G	25	6.5	0.7	5.4	1.7	0.0	6.1
Sample H	12	0.3	2.3	5.7	0.6	2.5	5.1
Sample I	16	1.4	3.2	14	6.8	4.0	1.4
Sample J	10	0.0	2.0	5.0	2.3	3.7	6.3
Average	14	2.2	1.8	9.4	4.5	3.8	4.5

It is clear from the two tables this comparison is not ideal. The Quasi-Optical, Perturbed Resonators, and SPDR techniques have the electric field oriented in the same plane as the dielectric under test. The Bereskin technique has the electric field oriented normal to the plane of the dielectric under test. The microstrip techniques have the electric field oriented almost normal to the plane of the dielectric under test, but not as well oriented as in a stripline structure. Each method also operates over different frequencies. Given the change in ϵ_r with frequency the comparison shown in Table 9 is not descriptive enough to provide a full picture. To more fully evaluate each method, they were also considered at a fixed value near 10 GHz since ϵ_r values are quoted at this frequency in data sheets. Table 10 shows the comparison of each method at 10 GHz. The impedance extraction technique is not included since a long pulse (200 ps) was used which makes the effective frequency much less than 10 GHz. The perturbed rectangular resonator was the one used at 10 GHz, so this is specified in the data table. The other methods, sans the quasi optical, all have frequency dependent operation at or near 10 GHz.

Table 10 – Measured Relative Permittivity at 10 GHz

Sample Name	Group Delay	Differential Phase Length	Rectangular Resonator	SPDR	Bereskin Stripline	Data Sheet
Sample A	3.25	3.27	3.46	3.448	3.08	3.3
Sample B	2.43	2.58	2.87	2.789	2.46	2.5
Sample C	2.95	3.12	3.39	3.317	2.90	3.00
Sample D	3.28	3.51	3.43	3.445	3.28	3.50
Sample E	2.18	2.22	2.29	2.260	2.17	2.20
Sample F	3.72	3.62	3.72	3.577	3.36	3.6
Sample G	2.71	2.94	2.89	2.991	2.76	2.94
Sample H	3.45	3.57	3.53	3.424	3.32	3.50
Sample I	2.22	2.25	2.34	2.297	2.17	2.20
Sample J	2.98	3.05	2.95	2.894	2.81	3.00

Once the methods were all compared at 10 GHz a percent difference was calculated against the data sheet. Table 11 shows the percent difference. Again, the quasi optical method was not considered in this evaluation. It became immediately clear from this comparison that differential phase length and group delay methods provided values closest to the data sheet values specified. The Bereskin stripline method gave values quite close to the values provided in the data sheets. The methods with the electric field oriented in the plane of the dielectric were most different from the data sheet values. This is not surprising since the data sheet values are generally based stripline (normal) permittivity values.

Table 11 – Percent Difference of Measured versus Expected Relative Permittivity at 10 GHz

Sample Name	Group Delay	Differential Phase Length	Rectangular Resonator	SPDR	Bereskin Stripline
Sample A	1.5	0.9	4.8	4.5	6.7
Sample B	2.8	3.2	15	12	1.6
Sample C	1.7	4.0	13	11	3.3
Sample D	6.3	0.3	2.0	1.6	6.3
Sample E	0.9	0.9	4.1	2.7	1.4
Sample F	3.3	0.6	3.3	0.6	6.7
Sample G	7.8	0.0	1.7	1.7	6.1
Sample H	1.4	2.0	0.9	2.2	5.1
Sample I	0.9	2.3	6.4	4.4	1.4
Sample J	0.7	1.7	1.7	3.5	6.3
Average	2.7	1.6	5.3	4.4	3.9

Table 12 shows the group delay method, differential phase length method, and open resonator from 3 GHz to 40 GHz. These methods were chosen for comparison due to their operation over this band as a way of better comparing each method. The resonant method does not provide the same resolution with regard to frequency as the transmission and reflection approaches. Hence, four frequencies were chosen for consideration, 3 GHz, 10 GHz, 26 GHz, and 40 GHz. At 3 GHz and 10 GHz, the perturbed resonator is the rectangular cavity. At 26 GHz and 40 GHz, the perturbed resonator is the open resonator cavity.

Table 12 – Comparison of Frequency Dependent Methods 3-40 GHz

Sample Name	Group Delay				Differential Phase Length				Open Resonator			
	3 GHz	10 GHz	26 GHz	40 GHz	3 GHz	10 GHz	26 GHz	40 GHz	3 GHz	10 GHz	26 GHz	40 GHz
Sample A	3.28	3.25	3.27	3.34	3.29	3.27	3.26	3.25	3.46	3.46	3.42	3.41
Sample B	2.42	2.43	2.5	2.53	2.55	2.53	2.51	2.51	2.88	2.87	2.80	2.80
Sample C	2.97	2.95	3.01	3.04	3.15	3.12	3.09	3.08	3.39	3.39	3.39	3.39
Sample D	3.27	3.28	3.35	3.36	3.54	3.51	3.49	3.49	3.42	3.43	3.46	3.45
Sample E	2.12	2.18	2.14	2.32	2.23	2.22	2.21	2.21	2.29	2.29	2.25	2.24
Sample F	3.72	3.72	3.78	3.91	3.65	3.62	3.60	3.59	3.72	3.72	3.61	3.59
Sample G	2.71	2.71	2.79	2.82	2.98	2.94	2.93	2.92	2.89	2.89	2.93	2.91
Sample H	3.46	3.45	3.50	3.53	3.61	3.57	3.55	3.54	3.54	3.53	3.53	3.53
Sample I	2.21	2.22	2.23	2.31	2.26	2.25	2.24	2.24	2.34	2.34	2.37	2.36
Sample J	2.95	2.98	3.00	3.07	3.08	3.05	3.04	3.03	2.95	2.95	2.94	2.93

An additional breakdown of methods versus frequency was accomplished from 40 GHz to 60 GHz. The quasi optical method was considered against the differential phase length and open resonator methods. Table 13 presents the information at four frequencies, 40 GHz, 50 GHz, 56 GHz, and 60 GHz. This was done due to the resonant methods limitations.

Table 13 – Comparison of Methods from 40-60 GHz

Sample Name	Quasi Optical				Differential Phase Length				Open Resonator			
	40 GHz	50 GHz	56 GHz	60 GHz	40 GHz	50 GHz	56 GHz	60 GHz	40 GHz	50 GHz	56 GHz	60 GHz
Sample A	3.9	4.0	3.9	4.0	3.25	3.25	3.25	3.24	3.41	3.41	3.40	3.40
Sample B	2.0	2.0	2.0	1.9	2.51	2.50	2.50	2.50	2.80	2.79	2.78	2.78
Sample C	3.2	3.2	3.1	3.0	3.08	3.07	3.07	3.07	3.39	3.39	3.38	3.38
Sample D	3.3	3.4	3.3	3.2	3.49	3.49	3.49	3.49	3.45	3.44	3.42	3.42
Sample E	2.5	2.5	2.5	2.4	2.21	2.21	2.21	2.21	2.24	2.23	2.22	2.10
Sample F	3.8	3.9	3.8	3.8	3.59	3.59	3.59	3.58	3.59	3.56	3.54	3.52
Sample G	3.0	3.1	3.2	3.0	2.92	2.92	2.92	2.91	2.91	2.89	2.88	2.87
Sample H	3.8	3.9	3.8	3.9	3.54	3.53	3.53	3.52	3.53	3.52	3.51	3.51
Sample I	2.5	2.6	2.6	2.5	2.24	2.24	2.24	2.24	2.36	2.36	2.36	2.36
Sample J	3.2	3.3	3.3	3.1	3.03	3.03	3.03	3.03	2.93	2.93	2.92	2.92

Table 14 compares permittivity measurements from the Bereskin and SPDR methods against the perturbed resonator. At 10 GHz, the perturbed resonator is the rectangular cavity. At 26 GHz, the perturbed resonator is the open resonator cavity.

Table 14 – Relative Permittivity for Resonant Methods @ 10 GHz & 20 GHz

Sample Name	Rect.	Open	SPDR		Bereskin Stripline	
	10 GHz	26 GHz	10 GHz	20 GHz	10 GHz	20 GHz
Sample A	3.46	3.42	3.448	3.440	3.07	3.09
Sample B	2.87	2.80	2.789	2.787	2.46	2.47
Sample C	3.39	3.39	3.317	3.308	2.89	2.89
Sample D	3.43	3.46	3.445	3.436	3.27	3.30
Sample E	2.29	2.25	2.260	2.254	2.17	2.17
Sample F	3.72	3.61	3.577	3.568	3.36	3.36
Sample G	2.89	2.93	2.991	2.893	2.76	2.77
Sample H	3.53	3.53	3.424	3.402	3.31	3.33
Sample I	2.34	2.37	2.297	2.281	2.17	2.18
Sample J	2.95	2.94	2.894	2.883	2.81	2.82

Most of the techniques did not directly measure loss tangent. Table 15 summarizes the loss tangent measurements at 10 GHz. In general, the Bereskin method yields loss tangent values closest to the data sheet values.

Table 15 – Resonant Method Loss Tangent @ 10 GHz

Sample Name	Rectangular Resonator	SPDR	Bereskin Stripline	Data Sheet
Sample A	0.0025	0.0017	0.0032	0.0040
Sample B	0.0033	0.0016	0.0023	0.0020
Sample C	0.0013	0.0018	0.0021	0.0016
Sample D	0.0021	0.0025	0.0026	0.0028
Sample E	0.0008	0.0007	0.0009	0.0009
Sample F	0.0008	0.0008	0.0008	0.0015
Sample G	0.0014	0.0011	0.0013	0.0012
Sample H	0.0027	0.0023	0.0019	0.0020
Sample I	0.0021	0.0014	0.0009	0.0009
Sample J	0.0012	0.0017	0.0014	0.0011

Table 16 presents the loss tangent values at 20 GHz. Note that the lowest frequency reported for the open resonator was 26 GHz. The approximate values reported were interpolated based on the 26 GHz open resonator data and the 10 GHz rectangular cavity data.

Table 16 – Resonant Method Loss Tangent @ 20 GHz

Sample Name	Open Resonator (approx.)	SPDR	Bereskin Stripline	Data Sheet
Sample A	0.0023	0.0027	0.0033	0.0040
Sample B	0.0039	0.0020	0.0027	0.0020
Sample C	0.0019	0.0025	0.0024	0.0016
Sample D	0.0025	0.0041	0.0030	0.0028
Sample E	0.0005	0.0015	0.0008	0.0009
Sample F	0.0007	0.0020	0.0012	0.0015
Sample G	0.0010	0.0024	0.0024	0.0012
Sample H	0.0023	0.0038	0.0019	0.0020
Sample I	0.0018	0.0019	0.0009	0.0009
Sample J	0.0012	0.0024	0.0016	0.0011

Conclusions

Transmission line methods have the capability of measuring relative permittivity in a robust, repeatable way even at frequencies higher than 20 GHz. Unfortunately, there is no straightforward technique to extract loss tangent from these transmission line methods. This is mainly due to the fact that there is no way to separate the effect of the conductor from the effect of the dielectric.

Methods utilizing resonant cavities are capable of providing precise measurements of loss tangent. The higher the Q of the cavity, the more precise the loss tangent can be measured. Unfortunately, these high-Q resonant cavities generally require more expertise and the measurement is more tedious. Permittivity measurements using these resonant cavities are oriented in the same plane as the dielectric, which is generally not how the electric field is oriented in most transmission line structures.

The Bereskin method is most similar to the incumbent clamped stripline method (IPC 2.5.5.5), but the practical upper bound of frequency for this structure is about 20 GHz.

The value of this work is a publically disclosed measurement set on commercially available low-loss materials. The methods performed were representative of common techniques used to compare permittivity and loss tangents at high frequencies. This work is not designed to promote one method over another. It is simply a basis to compare the level of variation that can be expected at frequencies above 1 GHz.

The main objective of this work was not to “judge” one of these methods as being “good” or “bad”. All of the methods are useful depending on equipment availability, time available to test, thickness of samples, and various other factors. The main value of this work is to report results of each method on a common set of sample material representative of what would be used at frequencies greater than 10 GHz. This work can be used as a building-block to build a common understanding across the industry and better develop standards.

Acknowledgements

The following companies contributed sample material to support this work:

- DuPont Electronics and Communications
- Rogers Corporation (Both Rogers Advanced Connectivity Solutions and Arlon material sets represented)
- Taconic Advanced Dielectrics Division
- Panasonic Electronic Materials
- Park Electrochemical Corporation

The following companies contributed test support and use of equipment for this work:

- Microstrip Transmission Line Methods. Extraction from impedance and group delay extraction – DuPont
- Microstrip Transmission Line Methods. Differential phase length – Rogers
- Free Space Transmission Method, Quasi-optical – Isola
- Rectangular cavity and open resonator – DuPont
- Split post dielectric resonator - SPDR – Rogers
- Bereskin resonator – Taconic

Sean Sweeny, a student at Binghamton University performed much of the testing at DuPont.

References

- [1] G. Oliver, "Characterization of Flexible Circuit Dielectrics for High Speed Applications," *DesignCon 2011*. Santa Clara, CA, 2011. <http://www.designcon.com>
- [2] IPC-TM-650-2.5.5.5 – Stripline Test for Permittivity and Loss Tangent (Dielectric Constant and Dissipation Factor) at X Band. <http://www.ipc.org>
- [3] ASTM-D-3380 - Standard Test Method for Relative Permittivity (Dielectric Constant) and Dissipation Factor of Polymer-Based Microwave Circuit Substrates1. <http://www.astm.org>
- [4] G. Oliver et al., "Comprehensive Analysis of Flexible Circuit Materials Performance in Frequency and Time Domains," *DesignCon 2012*. Santa Clara, CA, 2012. <http://www.designcon.com>
- [5] Polar Instruments. SI-9000 Impedance Calculation Tool. <http://www.polarinstruments.com>
- [6] Bahl, I., Bhartia, P., *Microwave Solid State Circuit Design*, Wiley, New York, 1988.
- [7] Group and Phase Delay Measurements with Vector Network Analyzer ZVR, Application Note. <http://www.rohde-schwarz.com>
- [8] D. Pozar, *Microwave Engineering*, 2nd ed, New York, Wiley, 1998.
- [9] J. Coonrod and G. Oliver, "Practical Measurements of Dielectric and Loss of PCB Materials at High Frequencies," *DesignCon 2014*. Santa Clara, CA, 2014. <http://www.designcon.com>
- [10] TK Instruments. Quasi-Optical Measurement Circuit for Agilent's VNA's. <http://www.terhertz.co.uk/>
- [11] IPC-TM-650-2.5.5.13 – Relative Permittivity and Loss Tangent Using a Split Cylinder Resonator. <http://www.ipc.org>
- [12] Oliver, Glenn, "Electrical Characterization of Flexible Circuit Materials at High Frequency," *DesignCon 2010*. Santa Clara, CA, 2010. <http://www.designcon.com>
- [13] Agilent Split Post Dielectric Resonators for Dielectric measurements of Substrates, Application Note. <http://www.agilent.com>
- [14] IPC-TM-650-2.5.5.5.1 – Stripline Test for Complex Relative Permittivity of Circuit Board Materials to 14 GHz. <http://www.ipc.org>
- [15] David L. Wynants, Sr., DK or Dielectric Constant or Relative Permittivity or ϵ_r : What is it, Why is it Important, and How Does Taconic Test for It? http://www.taconic-add.com/pdf/technicaltopics--dielectric_constant.pdf
- [16] United States Patents 5083088 & 5187443 <http://patft.uspto.gov/>

Round Robin of High Frequency Test Methods

Work Product of the IPC D-24C Task Group

Glenn Oliver, DuPont (Chair: IPC D-24C)

John Andresakis, Park Electrochemical

John Coonrod, Rogers Corp., (Vice Chair: IPC D-24C)

Don DeGroot, CCN

Chudy Nwachukwu, Isola

Jonathan Weldon, DuPont

David L. Wynants, Sr., Taconic

What is the IPC D-24C Task Group?

- Responsible for development of frequency domain test methods
 - Measurements usually performed with a Vector Network Analyzer (VNA)
 - Primary participants in this group are PCB material suppliers
 - Test labs, designers, and OEMs also participate and are encouraged to attend!
- Current areas of focus:
 - Dk and Df measurement over a wide frequency range (broadband)
 - Dk and Df measurement above 10 GHz

Purpose of This Project

- Keep the materials constant and determine the impact of different test methods
 - 10 different high frequency materials from the same lot from 5 different manufacturers
 - Same material tested at 5 locations using the test methods available that were either capable of a broad frequency range and/or measurement above 20 GHz
- Share the methods and results and compile for comparison
 - Dk and Df measurement over a wide frequency range (broadband)
 - Dk and Df measurement above 10 GHz

Some Details

- PCB Materials
 - Double-sided copper clad laminate (0.5 oz.)
 - Thickness 100-150 μm
 - $2.0 < Dk < 4.0$
 - $Df \leq 0.005$
 - All round robin samples from the same lot
- Testing
 - Have to test the PCB material by itself, not as a multilayer PCB
 - Test results should measure Dk and/or Df at frequencies higher than 10 GHz

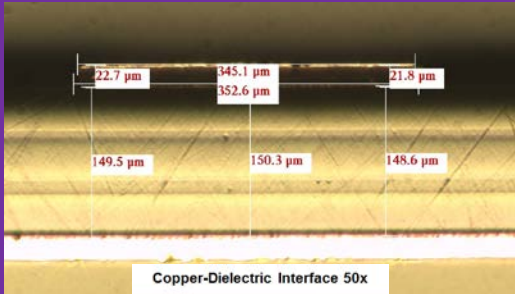
PCB Materials

Sample Name	Material Description	Expected Normal ϵ_r @ 10 GHz	Expected $\tan \delta$ @ 10 GHz	Nominal Thickness, mil (μm)
Sample A	Flex Polyimide	3.3	0.0040	6 (150)
Sample B	Flex Fluoropolymer / Polyimide Composite	2.5	0.0020	4 (100)
Sample C	Liquid Crystal Polymer (LCP)	3.00	0.0016	4 (100)
Sample D	Ceramic Filled Polymer on Fiberglass Substrate	3.50	0.0028	5 (125)
Sample E	Glass Microfiber Reinforced PTFE	2.20	0.0009	5 (125)
Sample F	Ceramic Filled PTFE	3.6	0.0015	5 (125)
Sample G	Micro Dispersed Ceramic in PTFE Composite on Woven Fiberglass Substrate	2.94	0.0012	5 (125)
Sample H	Ceramic filled PTFE on Woven Fiberglass Substrate	3.50	0.0020	5 (125)
Sample I	PTFE on Woven Fiberglass Substrate	2.20	0.0009	5 (125)
Sample J	Ceramic Filled PTFE on Fiberglass Substrate	3.00	0.0011	5 (125)

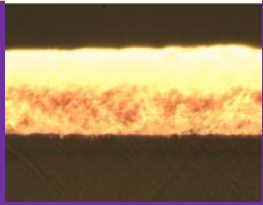
Cross Section Photos of Samples A-E

A

Unreinforced Polyimide

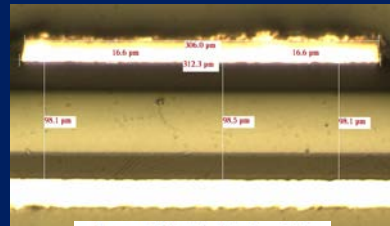


Copper-Dielectric Interface 50x

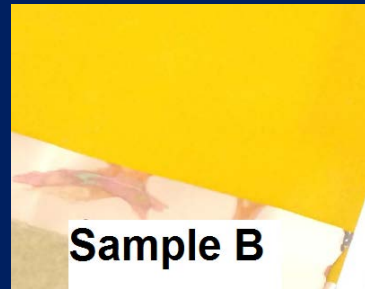
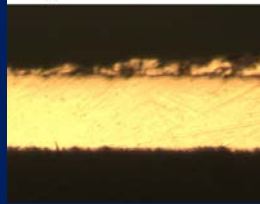


B

Unreinforced
Fluoropolymer /
Polyimide Composite

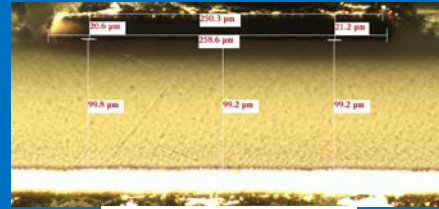


Copper-Dielectric Interface 50x

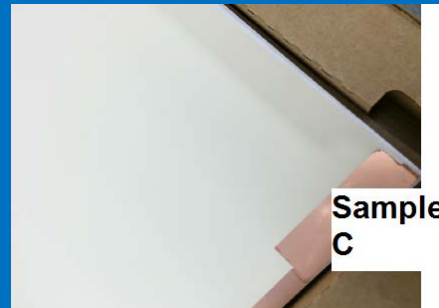
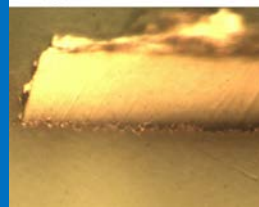


C

Unreinforced Liquid
Crystal Polymer

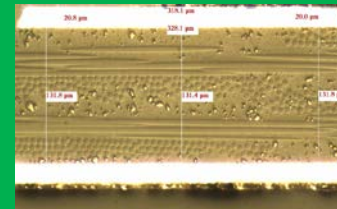


Copper-Dielectric Interface 50x

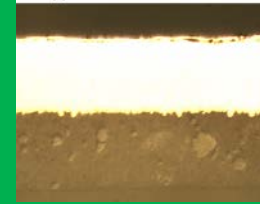


D

Ceramic Filled
Polymer on
Fiberglass Substrate

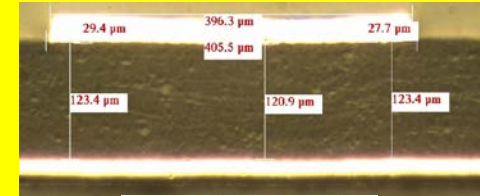


Copper-Dielectric Interface 50x

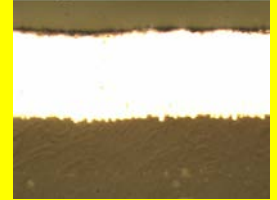


E

Glass Microfiber
Reinforced PTFE



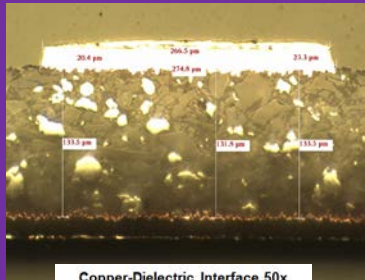
Copper-Dielectric Interface 50x



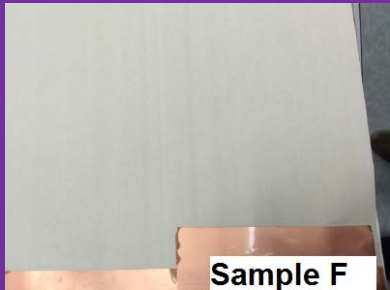
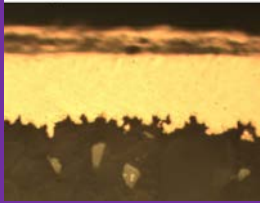
Cross Section Photos of Samples F-J

F

Ceramic Filled PTFE



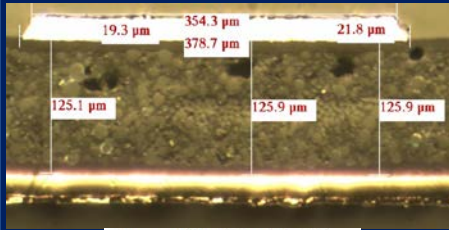
Copper-Dielectric Interface 50x



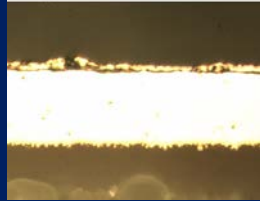
Sample F

G

Micro Dispersed Ceramic in PTFE Composite on Woven Fiberglass Substrate



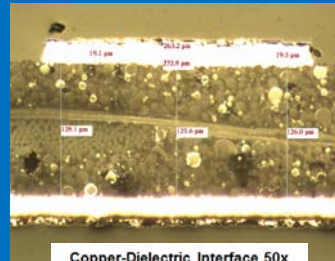
Copper-Dielectric Interface 50x



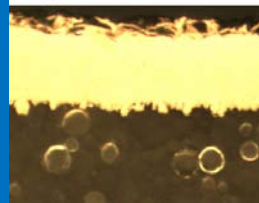
Sample G

H

Ceramic filled PTFE on Woven Fiberglass Substrate



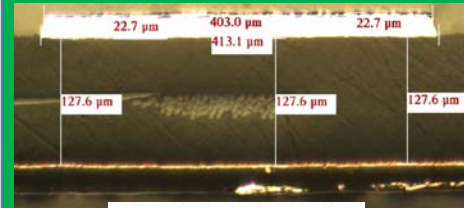
Copper-Dielectric Interface 50x



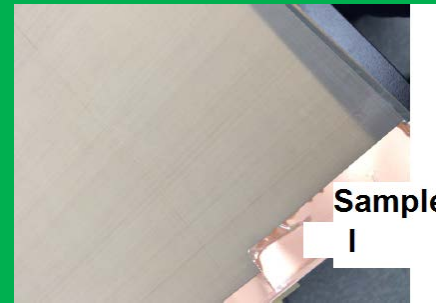
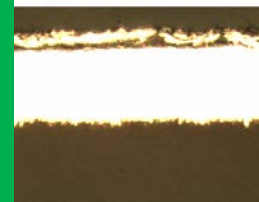
Sample H

I

PTFE on Woven Fiberglass Substrate



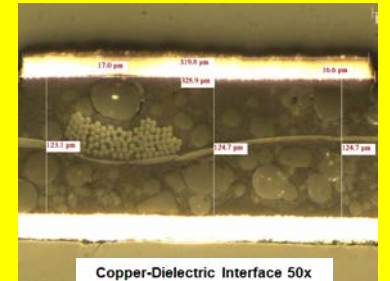
Copper-Dielectric Interface 50x



Sample I

J

Ceramic Filled PTFE on Fiberglass Substrate



Copper-Dielectric Interface 50x



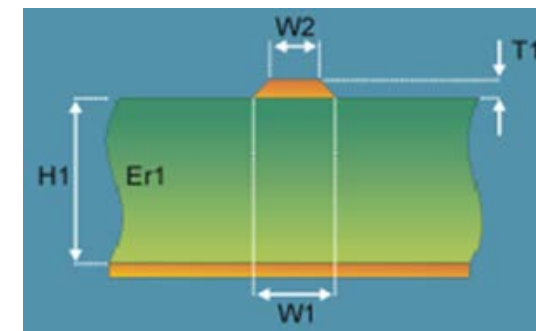
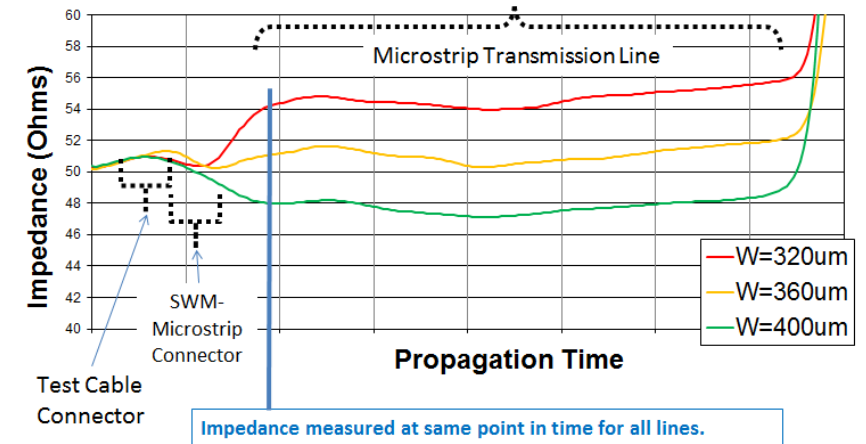
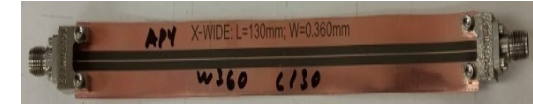
Sample J

Measurement Methods Performed

- Microstrip Transmission Line Methods:
 - Extraction from impedance (Dk only) [Oliver]
 - Group delay extraction from phase (Dk only) [Oliver]
 - Differential phase length (Dk only) [Coonrod]
- Free Space Transmission Method In-Plane of Dielectric:
 - Free space quasi-optical (Dk only) [Nwachukwu]
- Perturbed Resonant Cavities - Electric Field Oriented In-Plane of Dielectric:
 - Split Cylinder Resonator (Dk and Df) [DeGroot]
 - Rectangular cavity and open resonator (Dk and Df) [Oliver]
 - Split post dielectric resonator - SPDR (Dk and Df) [Coonrod]
- Coupled Stripline - Electric Field Oriented Normal to Plane of Dielectric:
 - Bereskin resonator (Dk and Df) [Wynants]

Normal Dk Extraction from TDR Zo Measurements

- Not a High Frequency Test Method!
 - Shown for reference as a “traditional” method that may be performed in PCB fabrication shops
- Microstrip lines made with Z near 50 ohms
 - Attempt to have $Z > 50$ ohms, $Z < 50$ ohms, $Z = 50$ ohms
 - Specifically, three widths x two lengths (130mm and 230 mm)
- Measure using TDR
 - Coax to microstrip connectors used in this cases but not required in general for Dk extraction
 - Select a specific time point for impedance measurement – center average not recommended for narrow lines
- Do physical measurements and back-calculate Dk
 - Average the impedance from the six lines and determine 50 ohm line width
 - Plug in physical measurements and solve for Dk (ϵ_r)



[Oliver]

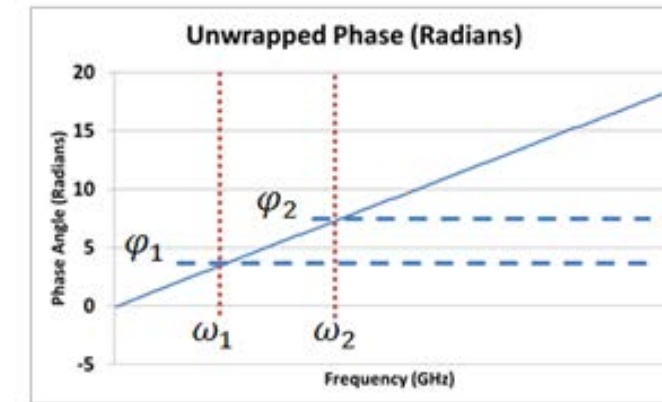
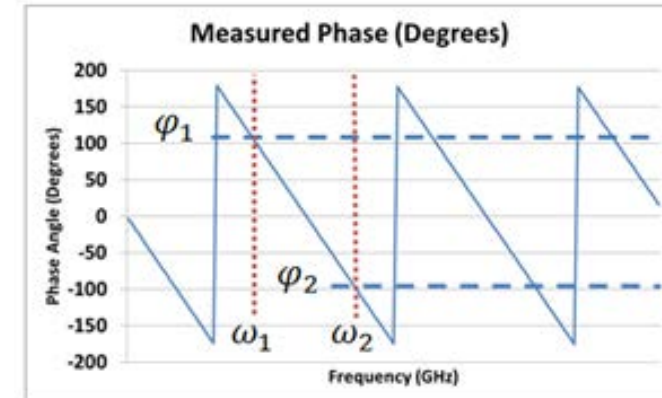
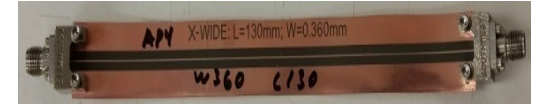
Normal Dk Extraction from Group Delay

- Use same microstrip lines created in previous method
- Measure S-Parameters of each
 - Specifically here, measure from 0.04 GHz to 40 GHz
- Unwrap phase
- Determine group delay
 - Eliminate effect of connectors by calculating group delay over difference of the two lines
- Calculate K_{eff}
- Calculate $E_r = Dk$

$$Group\ Delay\ (\tau_g) = \frac{\Delta\phi}{\Delta\omega} = \frac{\phi_2 - \phi_1}{\omega_2 - \omega_1}$$

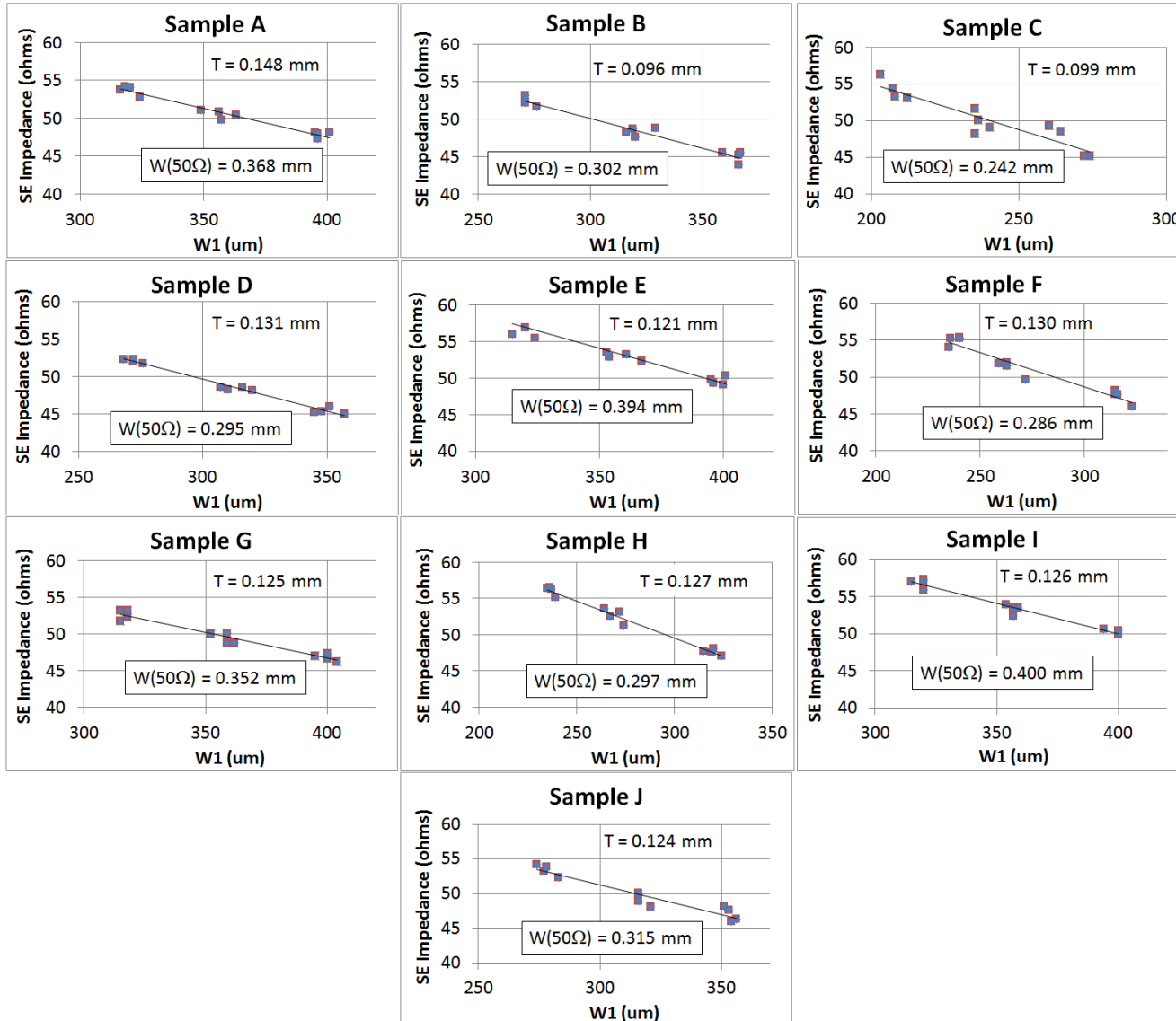
$$Effective\ Dielectric\ Constant\ (K_{eff}) = \left(\frac{c * \tau_g}{L}\right)^2$$

$$Relative\ Permittivity\ (\epsilon_r) = \frac{1 + (2 * K_{eff} - 1) * \sqrt{1 + 12 \frac{h}{w}}}{\sqrt{1 + 12 \frac{h}{w}}}$$



[Oliver]

Dk Extraction from Impedance Measurements - Data



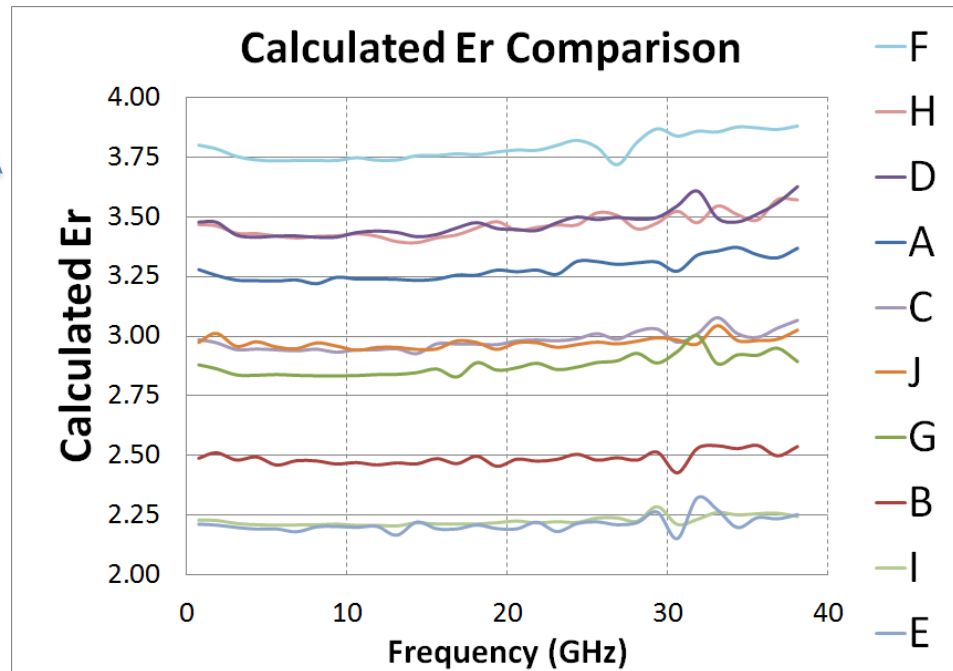
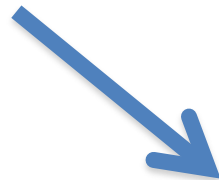
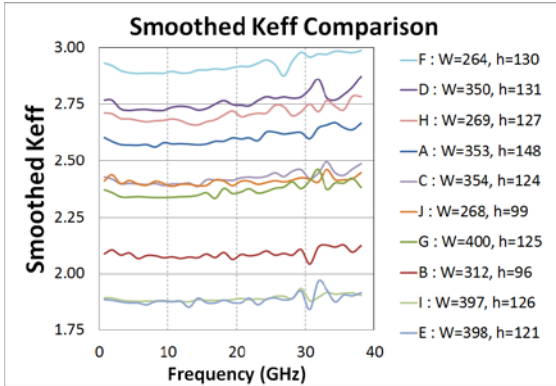
Sample	Datasheet Normal Dk @ 10 GHz	Extraction from TDR Zo
A	3.3	3.0
B	2.5	2.1
C	3	2.9
D	3.5	3.0
E	2.2	1.8
F	3.6	3.4
G	2.94	2.2
H	3.5	3.1
I	2.2	1.8
J	3	2.7

[Oliver]



Normal Dk Extraction from Group Delay - Data

Data in paper was more “choppy” due to IF bandwidth being set too high (1 kHz). Updated data is smoother since IF bandwidth is set to 10 Hz.



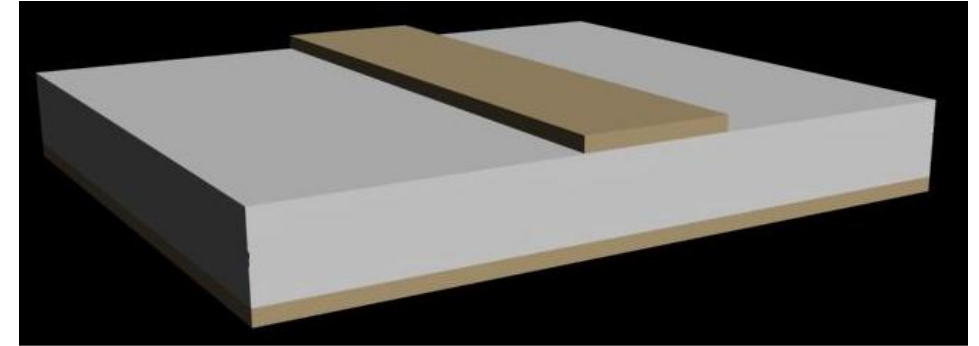
Sample	Expected Normal Dk @ 10 GHz	Extracted Normal Dk at 10 GHz
A	3.3	3.25
B	2.5	2.46
C	3	2.96
D	3.5	3.43
E	2.2	2.20
F	3.6	3.74
G	2.94	2.83
H	3.5	3.45
I	2.2	2.22
J	3	2.98

[Oliver]

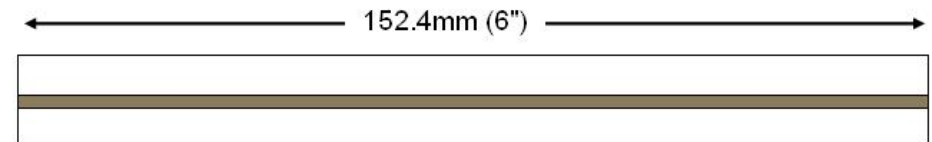


Microstrip Differential Phase Length Method

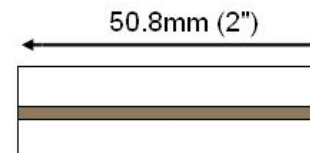
- Circuit test method, using microstrip transmission line circuits of two different lengths
- Evaluates mostly z-axis properties
- Microstrip differential length method
 - Determines insertion loss
 - Generates Dk vs. Frequency curves



3D view



Top View



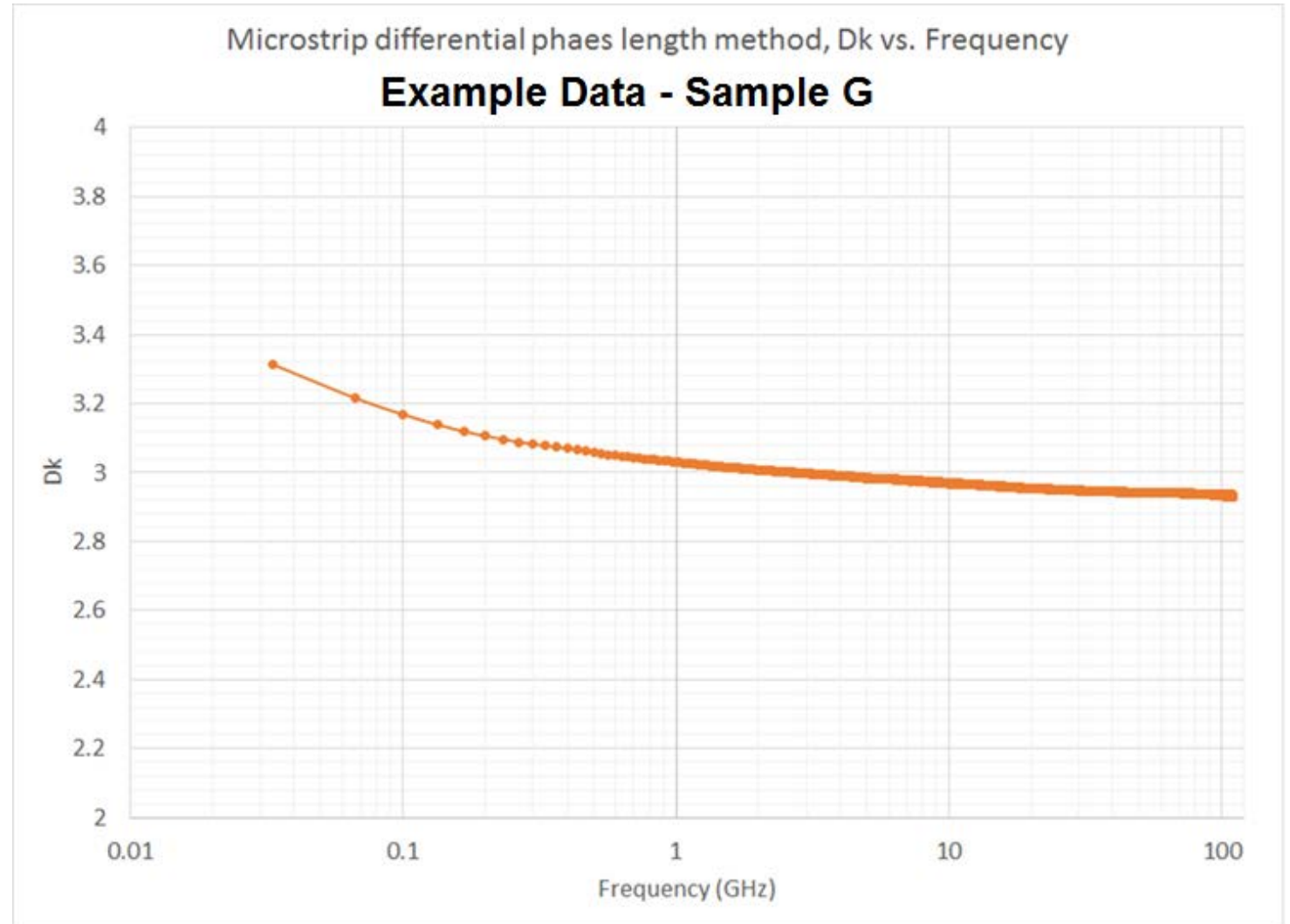
Top View

Substrate is ceramic filled PTFE.
Dielectric Constant is 10.2 per
IPC Clamped Stripline Test Method.
Substrate is 1.27mm (50mils) thick.
Copper is 18micron (1/2oz)
Electro-Deposited Copper.
Not shown to scale.

Source: This procedure is defined in a paper: “Two Methods for the Measurement of Substrate Dielectric Constant”, Nirod K. Das, Susanne M. Voda, and David Pozar, *IEEE Transactions on Microwave Theory and Techniques*, Vol MTT-35, No. 7, July 1987.

Microstrip Differential Phase Length Data

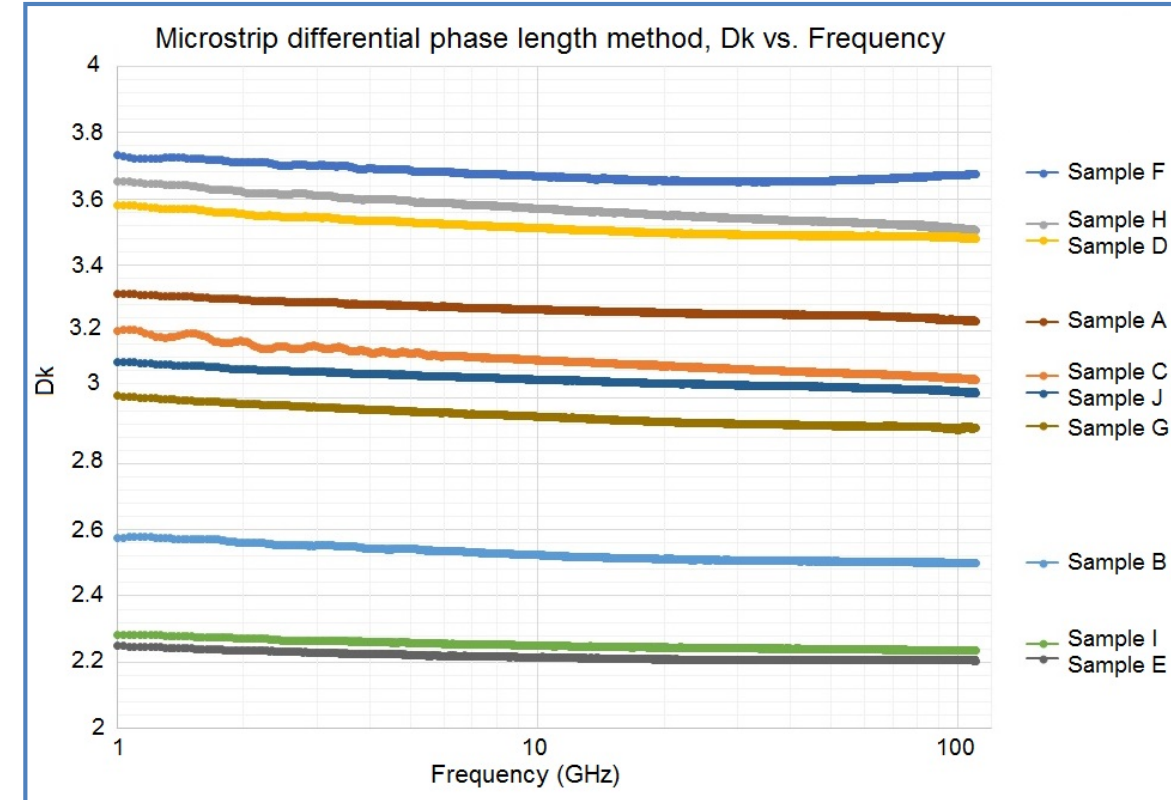
- Example of a very wideband measurement for Dk vs. Frequency



Microstrip Differential Phase Length Data

Table 1 –Circuit Board Materials Tested

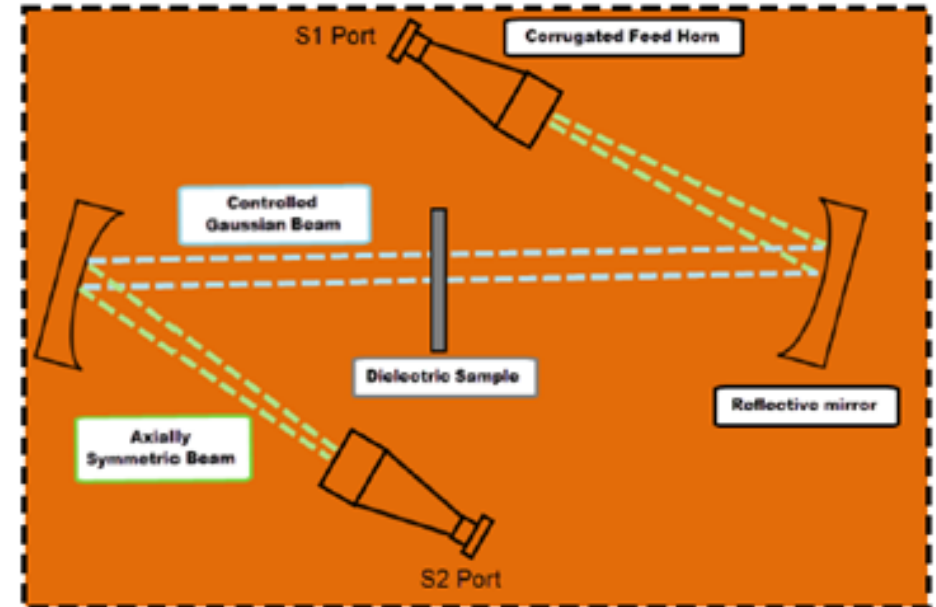
Sample Name	Material Description	Expected Normal ϵ_r @ 10 GHz	Expected $\tan \delta$ @ 10 GHz	Nominal Thickness, mil (μm)
Sample A	Flex Polyimide	3.3	0.0040	6 (150)
Sample B	Flex Fluoropolymer / Polyimide Composite	2.5	0.0020	4 (100)
Sample C	Liquid Crystal Polymer (LCP)	3.00	0.0016	4 (100)
Sample D	Ceramic Filled Polymer on Fiberglass Substrate	3.50	0.0028	5 (125)
Sample E	Glass Microfiber Reinforced PTFE	2.20	0.0009	5 (125)
Sample F	Ceramic Filled PTFE	3.6	0.0015	5 (125)
Sample G	Micro Dispersed Ceramic in PTFE Composite on Woven Fiberglass Substrate	2.94	0.0012	5 (125)
Sample H	Ceramic filled PTFE on Woven Fiberglass Substrate	3.50	0.0020	5 (125)
Sample I	PTFE on Woven Fiberglass Substrate	2.20	0.0009	5 (125)
Sample J	Ceramic Filled Epoxy on Fiberglass Substrate	3.00	0.0011	5 (125)



Quasi-Optical Free Space Measurement

- Freespace Quasi-optical measurement set-up
- Multiple Vendor dielectric sample thickness with *datasheet* DK / DF provided.
- Dielectric Permittivity characterization in 40 - 60 GHz frequency range.

- Quasi-Optical Measurement system (40 - 60 GHz)

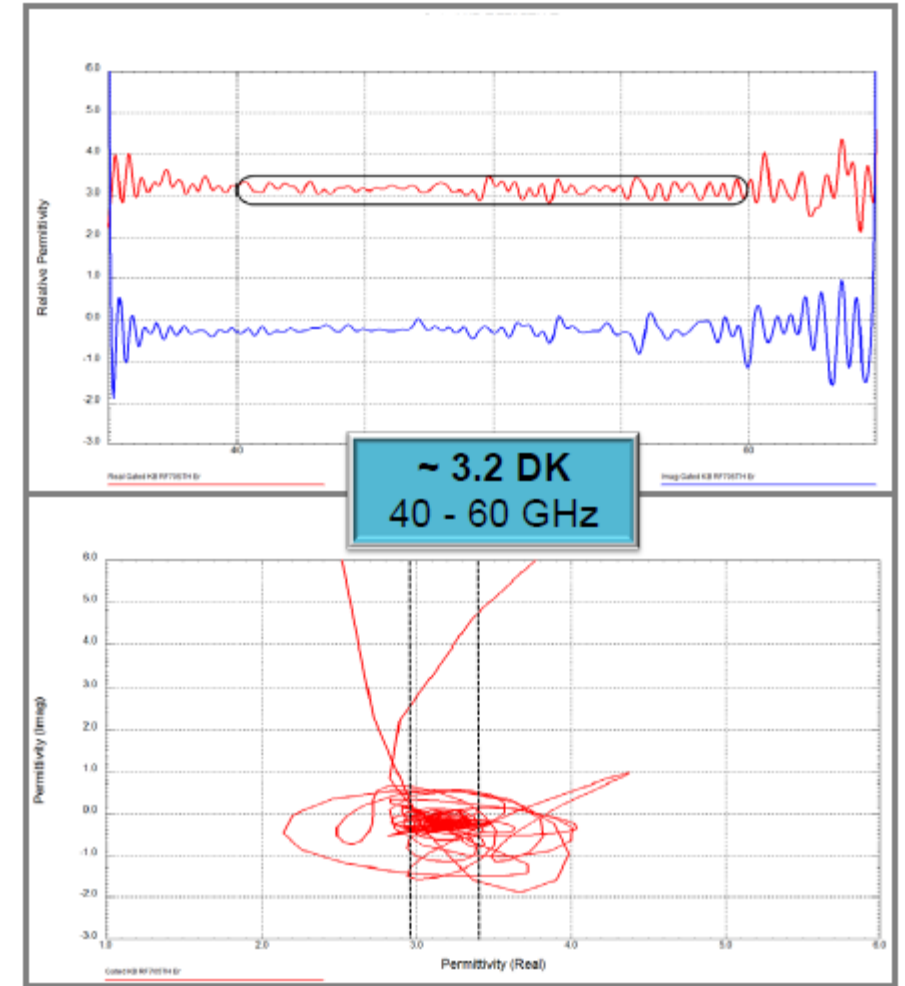


- Network Analyzer (10Hz IF bandwidth)
- Software (Calibration & TD Gating ~ 2ns)

Quasi-Optical Free Space Data

- Example analysis for Sample C
 - Dk
 - Cole-Cole plot

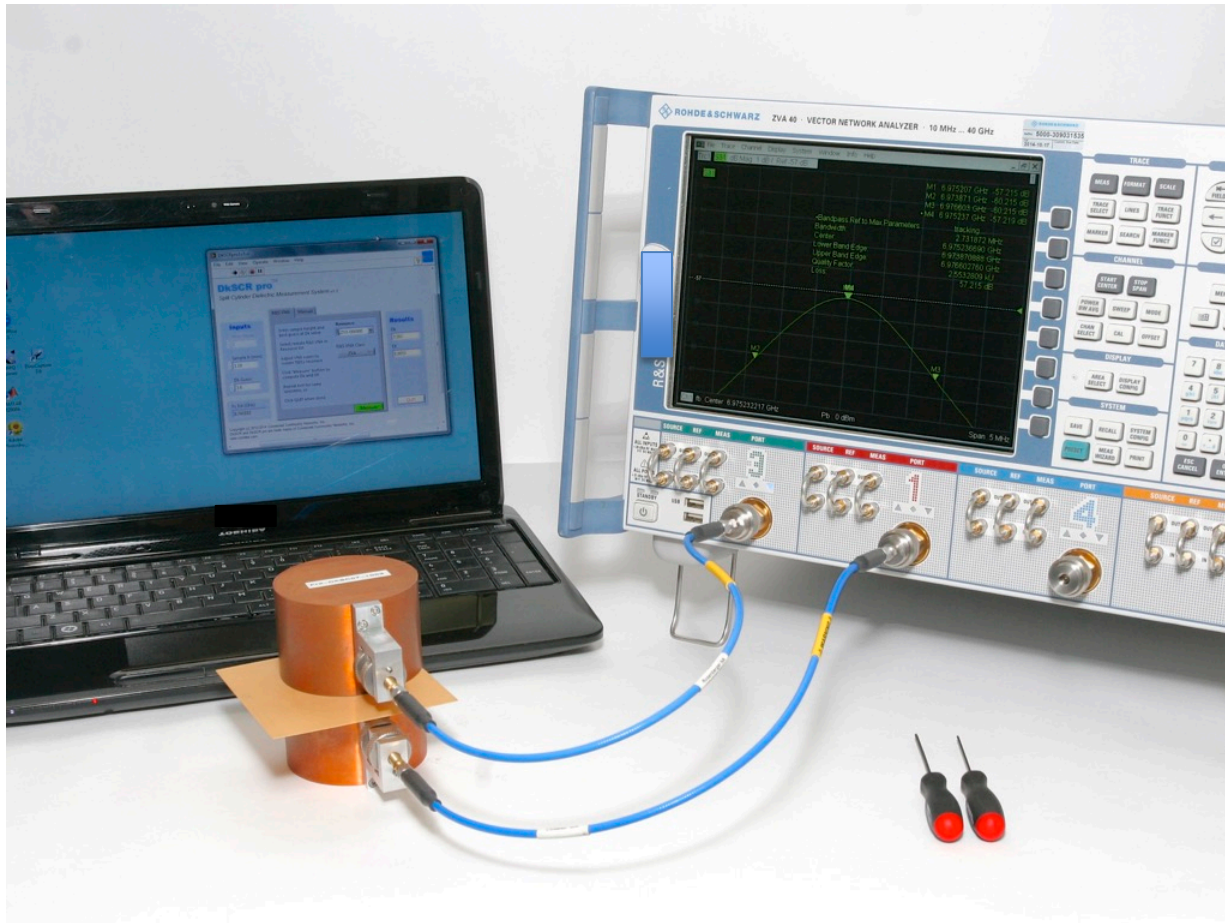
Sample	Quasi-Optical Free Space (Nwachukwu)
	40-60 GHz
A	3.9*
B	2.0
C	3.2
D	3.25
E	2.35
F	3.8
G	3.1
H	3.7
I	2.5
J	3.15



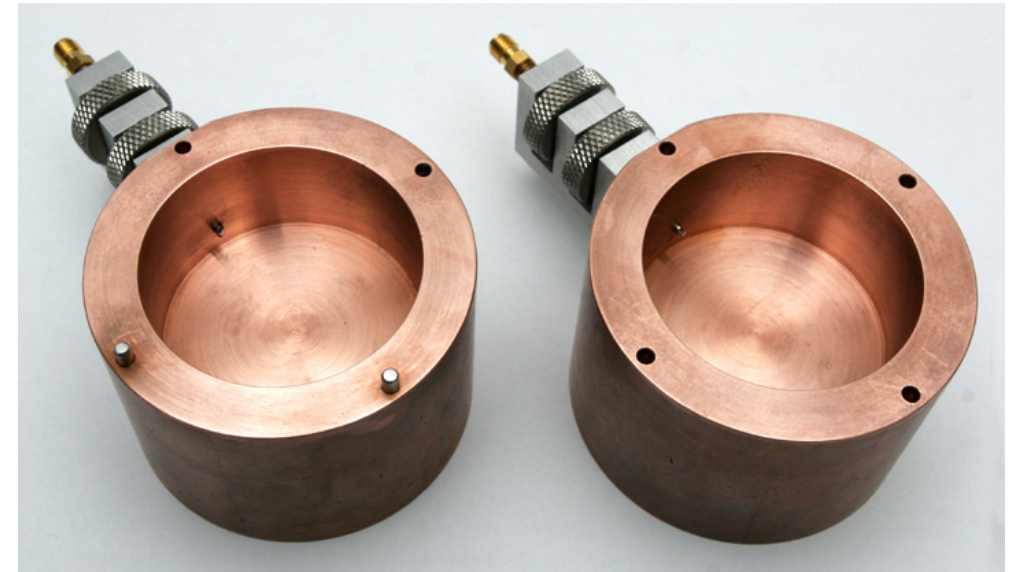
[Nwachukwu]

Split Cylinder Method for Dk and Df

NIST worked with IPC to create this method IPC TM-650 2.5.5.13



7 GHz Resonator
Coupler Adjustments
10 GHz & 24 GHz Resonators Available
In-Plane Dk

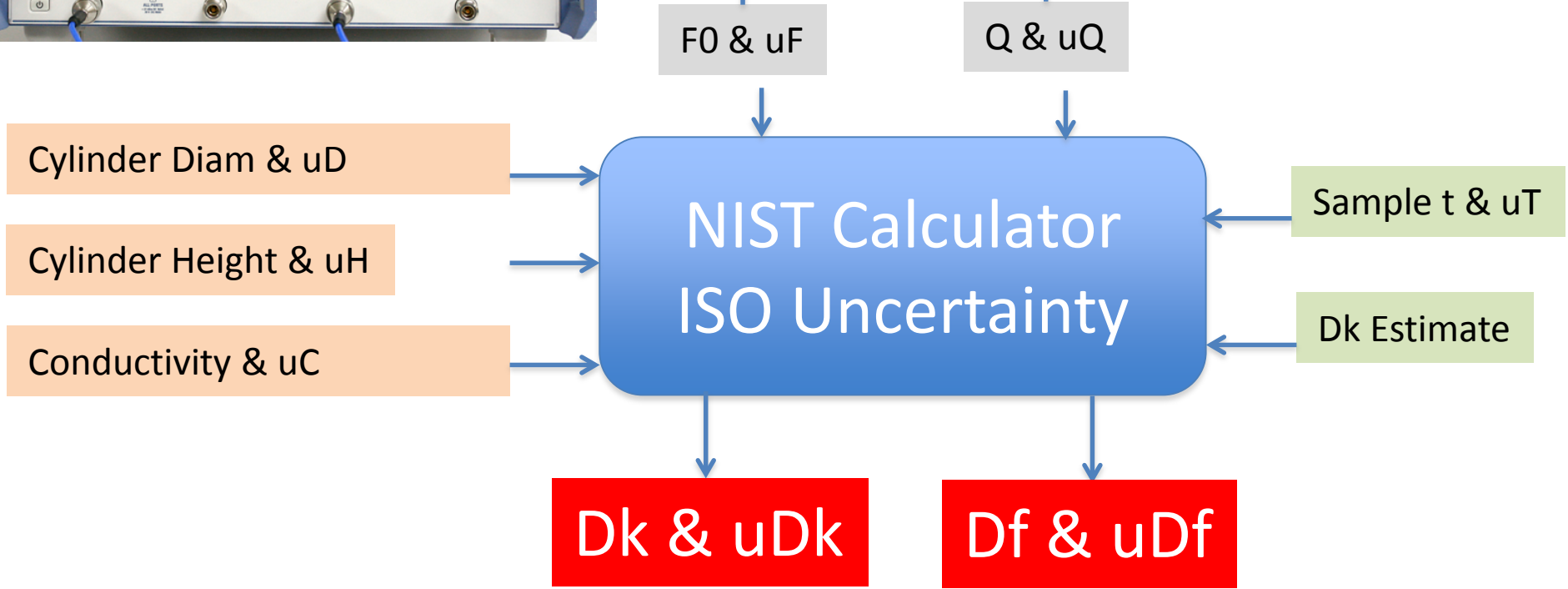
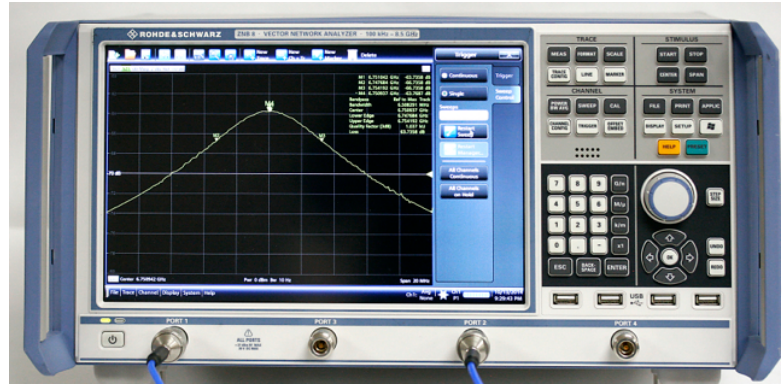


Split Cylinder Method for Dk and Df Thickness Measurements



- Sample is held in micrometer
- Vertical orientation
- Measured at least 5x over test region
- USB connection to production test software

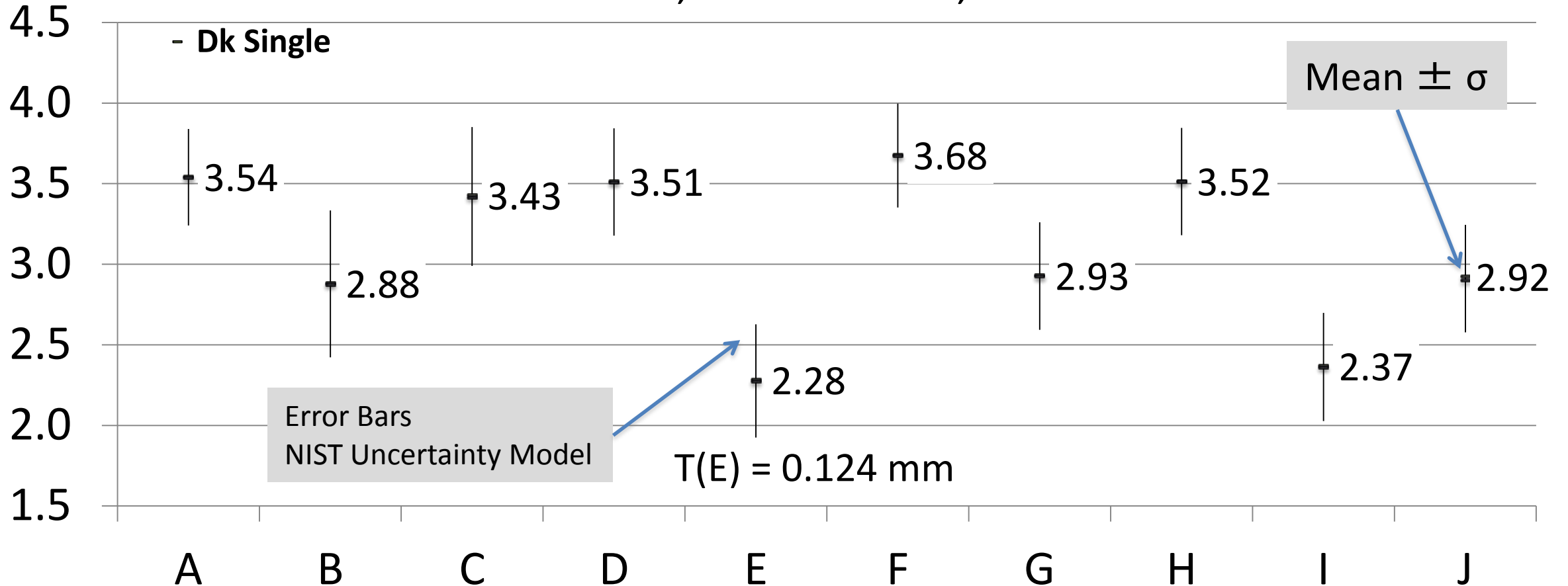
Split Cylinder Method for Dk and Df



Split Cylinder Method Dk Data of Single Layer

[DeGroot]

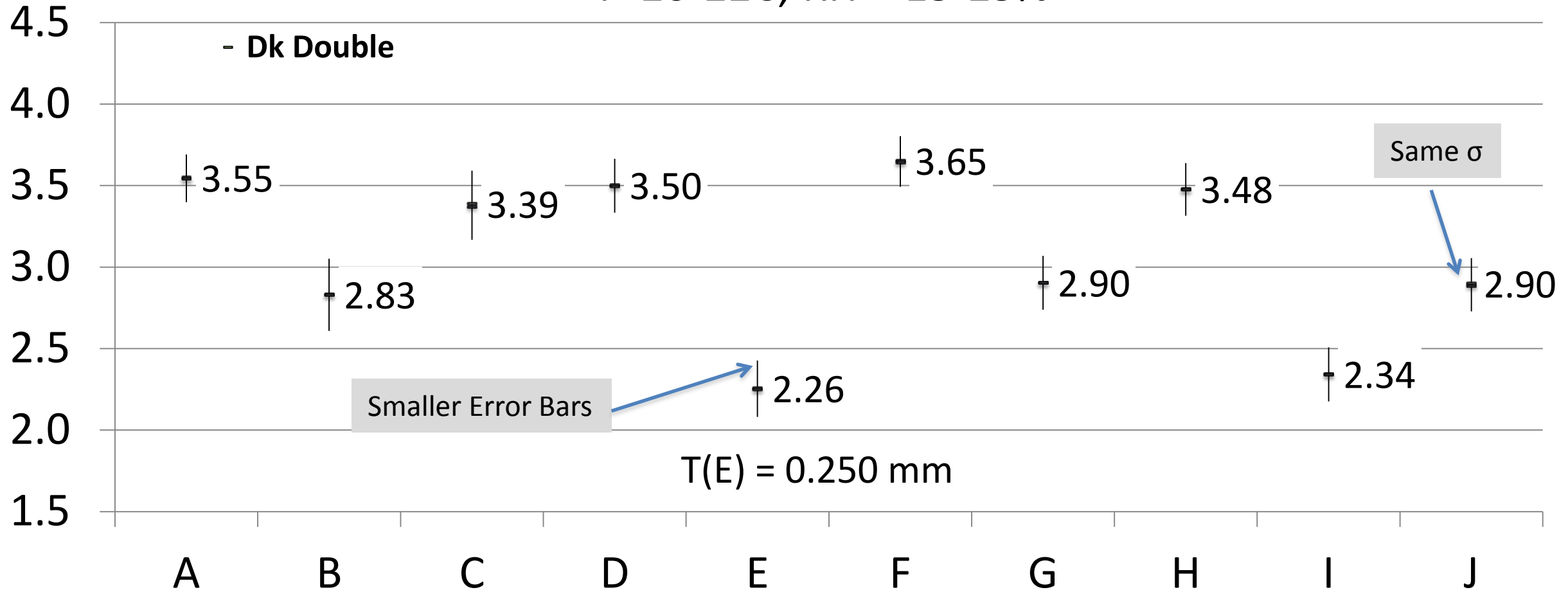
T=20-22C; RH = 30-40%, stored at RH=15-25%



Split Cylinder Method Dk Data of Double Layer

[DeGroot]

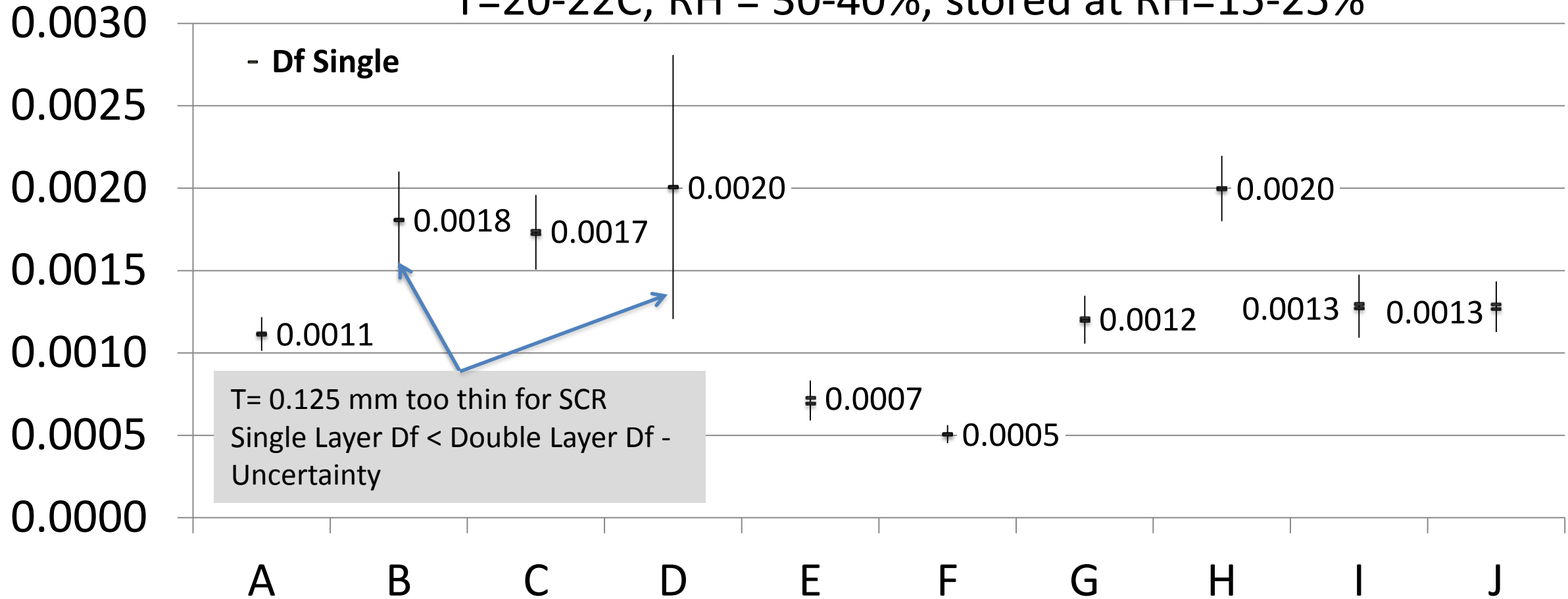
T=20-22C; RH = 15-25%



Split Cylinder Method Df Data of Single Layer

[DeGroot]

T=20-22C; RH = 30-40%, stored at RH=15-25%

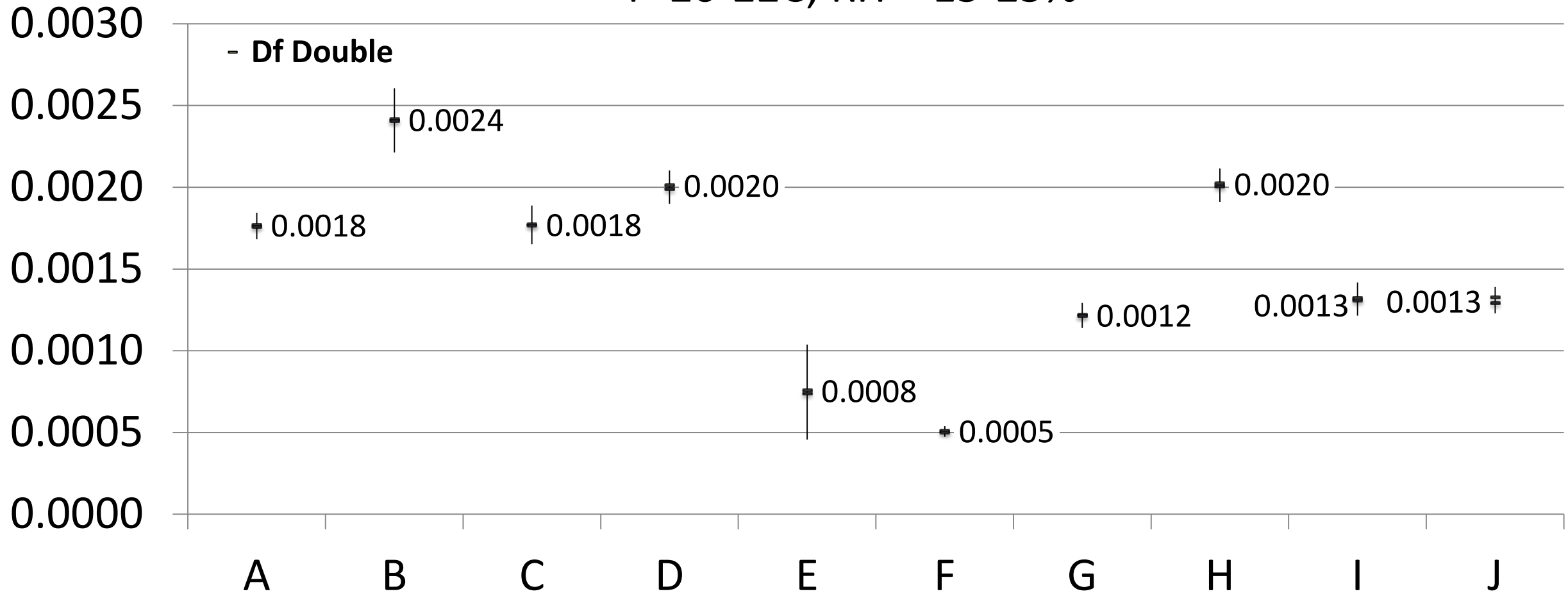




Split Cylinder Method Df of Double Layer

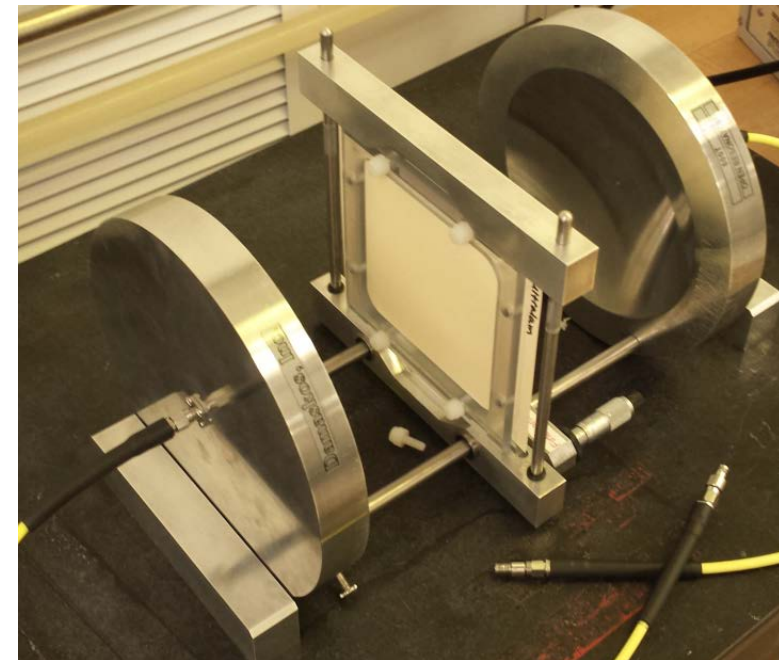
[DeGroot]

T=20-22C; RH = 15-25%



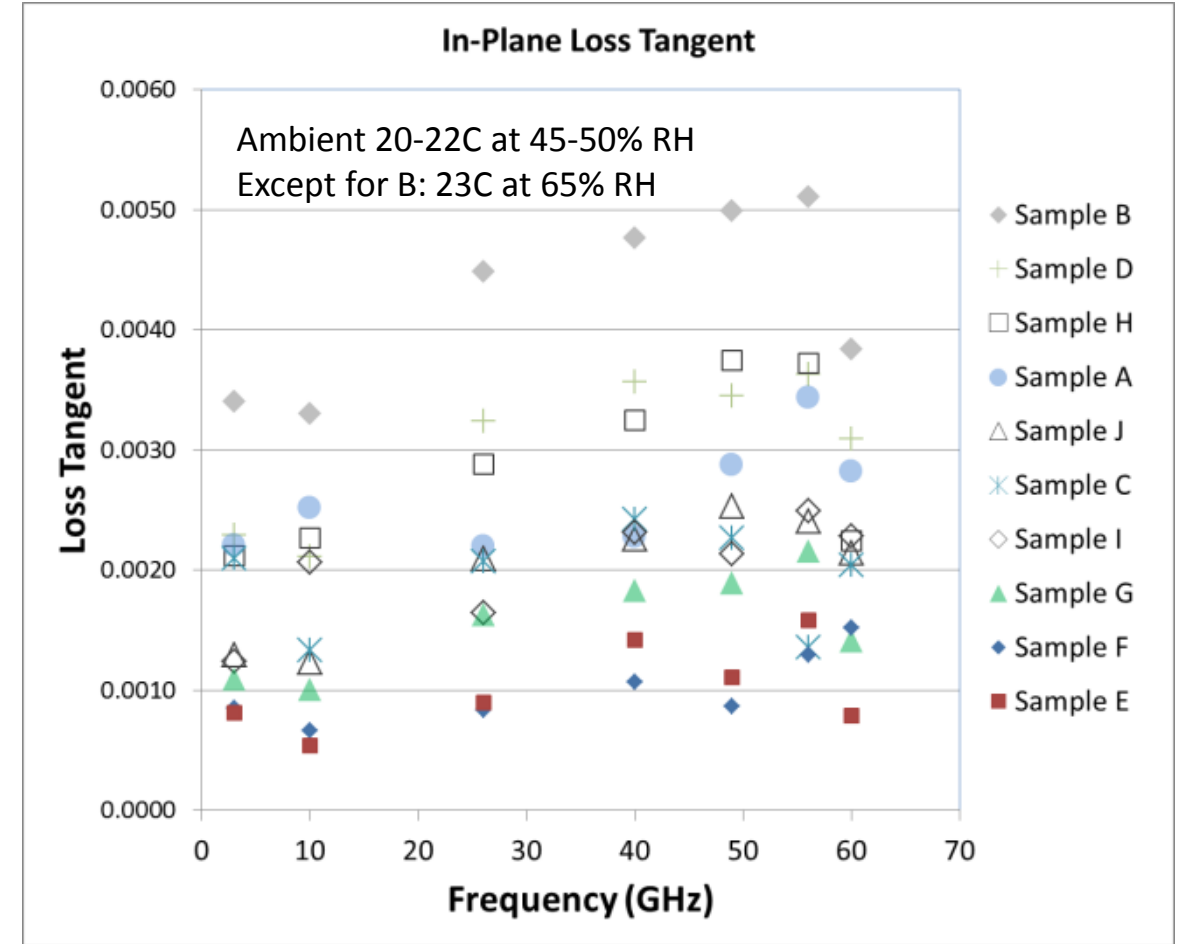
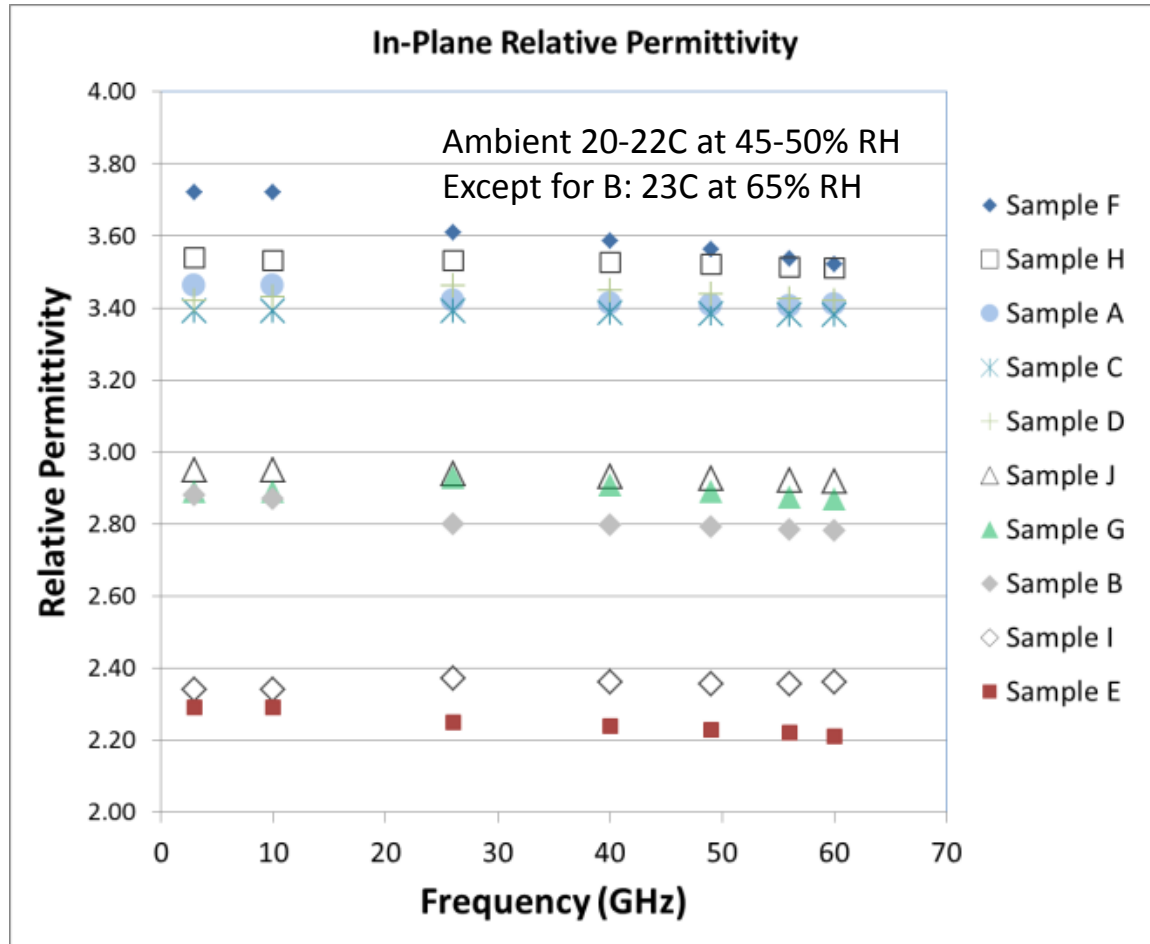
Df and In-Plane Dk – Resonant Cavities

- Perturbation methods – Measure the loaded and unloaded cavities and compare
 - Electric field oriented in the same plane as the dielectric
- Two Resonator Types
 - Rectangular cavity
 - Especially suited for thin dielectrics (<0.1 mm)
 - Six resonances between 2-11 GHz
 - Dk precision about 0.05; Df precision about 0.001
 - Open resonator
 - Resonance created by two mirrors
 - Can set to cavity lengths for various ranges 20-60 GHz
 - Precision better than 0.0001 for Df



[Oliver]

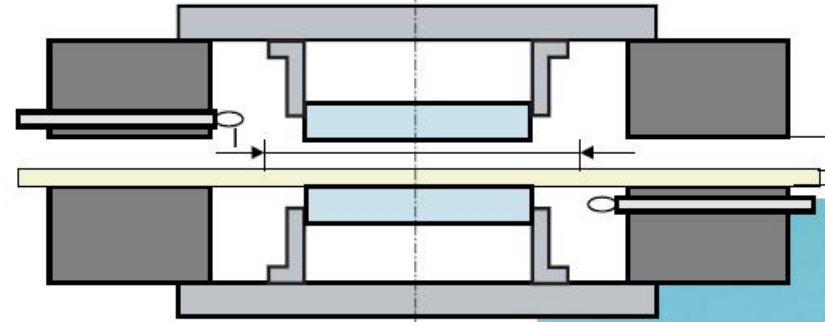
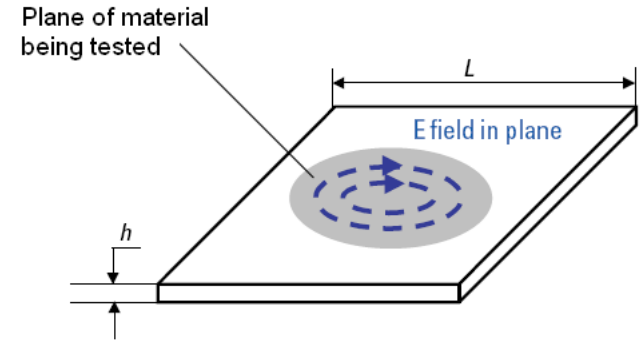
In-Plane Dk and Df – Resonant Cavity Data



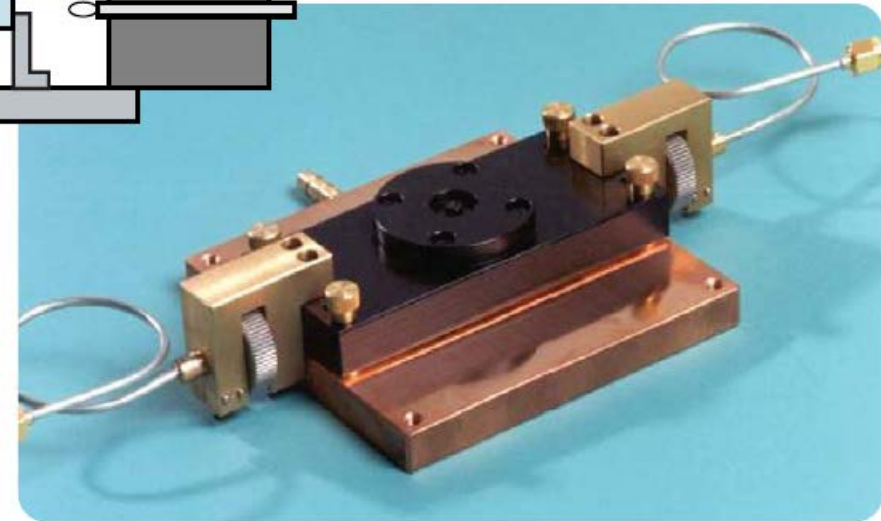
[Oliver]

Split Post Dielectric Resonator (SPDR)

- This is a raw material test
- Evaluates raw material (no copper effects) for Dk and Df in the x-y plane only
- SPDR fixtures tuned at:
 - 5 GHz
 - 10 GHz
 - 15 GHz
 - 20 GHz
- The combination of SPDR results and other z-axis test methods can give an indication for material anisotropy.



Test method definition:
[see Reference 1]



[Coonrod]

Split Post Dielectric Resonator Data

Table 1 –Circuit Board Materials Tested

Sample Name	Material Description	Expected Normal ϵ_r @ 10 GHz	Expected $\tan \delta$ @ 10 GHz	Nominal Thickness, mil (μm)
Sample A	Flex Polyimide	3.3	0.0040	6 (150)
Sample B	Flex Fluoropolymer / Polyimide Composite	2.5	0.0020	4 (100)
Sample C	Liquid Crystal Polymer (LCP)	3.00	0.0016	4 (100)
Sample D	Ceramic Filled Polymer on Fiberglass Substrate	3.50	0.0028	5 (125)
Sample E	Glass Microfiber Reinforced PTFE	2.20	0.0009	5 (125)
Sample F	Ceramic Filled PTFE	3.6	0.0015	5 (125)
Sample G	Micro Dispersed Ceramic in PTFE Composite on Woven Fiberglass Substrate	2.94	0.0012	5 (125)
Sample H	Ceramic filled PTFE on Woven Fiberglass Substrate	3.50	0.0020	5 (125)
Sample I	PTFE on Woven Fiberglass Substrate	2.20	0.0009	5 (125)
Sample J	Ceramic Filled Epoxy on Fiberglass Substrate	3.00	0.0011	5 (125)

SPDR results are from measurements of the x-y plane of the material

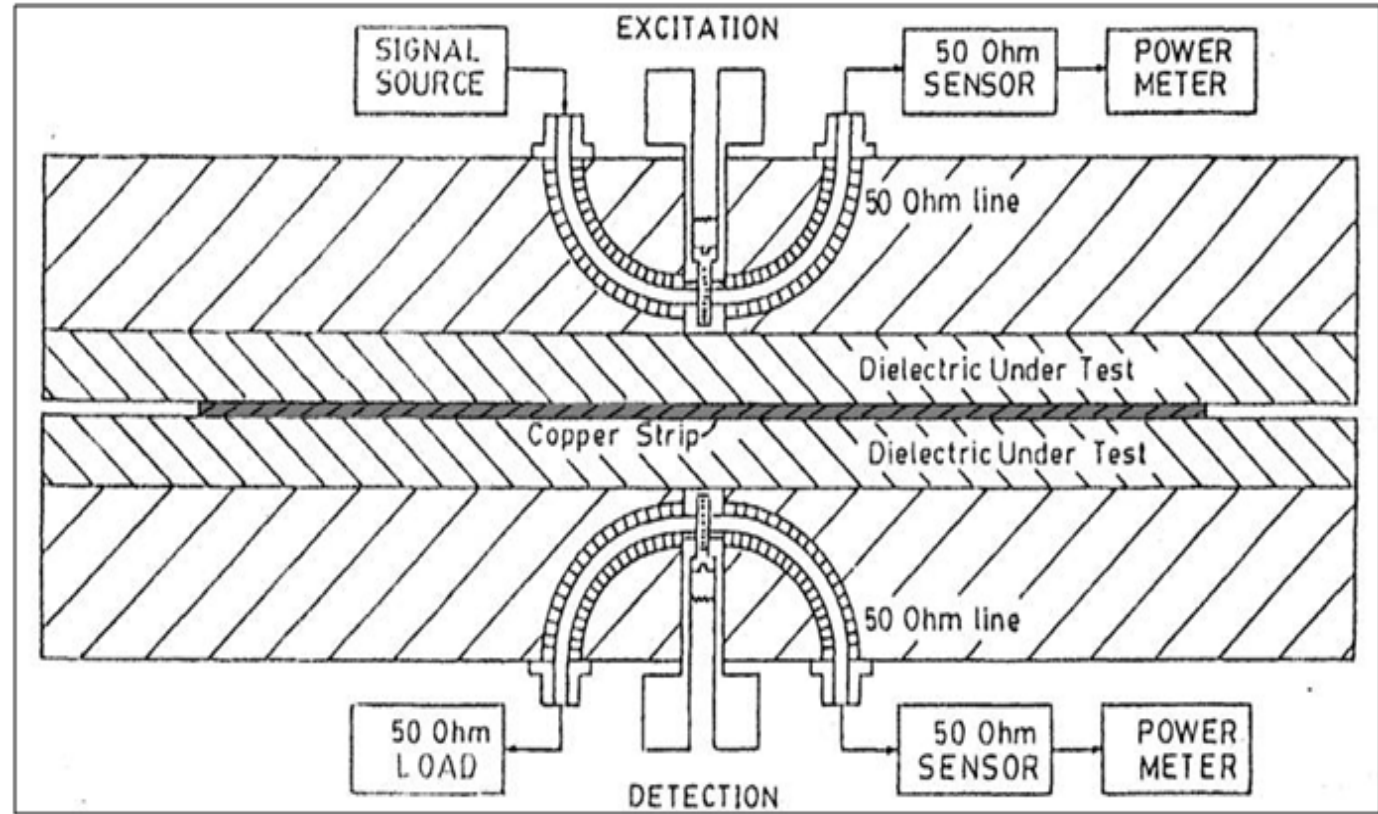
Most ϵ_r (Dk) and $\tan \delta$ (Df) values on data sheets are from z-axis measurements

Split Post Dielectric Resonator (SPDR)

	10 GHz		20 GHz	
	Dk	Df	Dk	Df
Sample A	3.448	0.0017	3.440	0.0027
Sample B	2.789	0.0016	2.787	0.0020
Sample C	3.317	0.0018	3.308	0.0025
Sample D	3.445	0.0025	3.436	0.0041
Sample E	2.260	0.0007	2.254	0.0015
Sample F	3.577	0.0008	3.568	0.0020
Sample G	2.991	0.0011	2.893	0.0024
Sample H	3.424	0.0023	3.402	0.0038
Sample I	2.297	0.0014	2.281	0.0019
Sample J	2.894	0.0017	2.883	0.0024

Bereskin Clamped Stripline Resonator

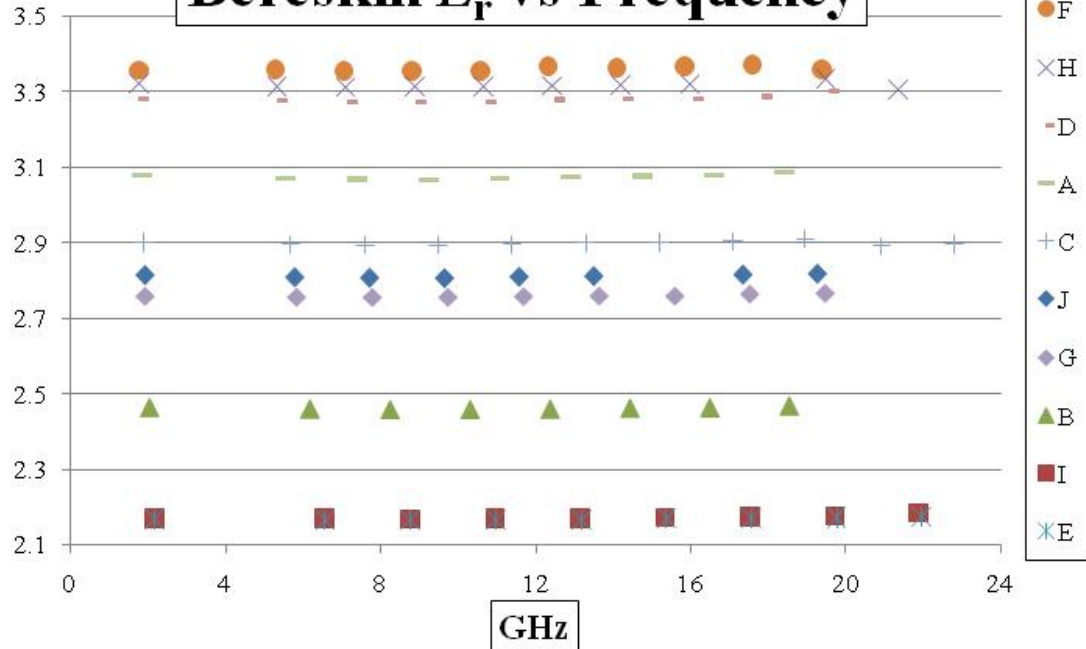
- 2 pcs/stacks
1.3125" X 4" > 11 mils
- Prefer 2-60 mil pcs
- Material supplied 4, 5, & 6 mils
- 2-15 pcs, 2-12 pcs, 2-10 pcs
- Everybody with equally undesirable conditions



[Wynants]

Bereskin Clamped Stripline Resonator Data

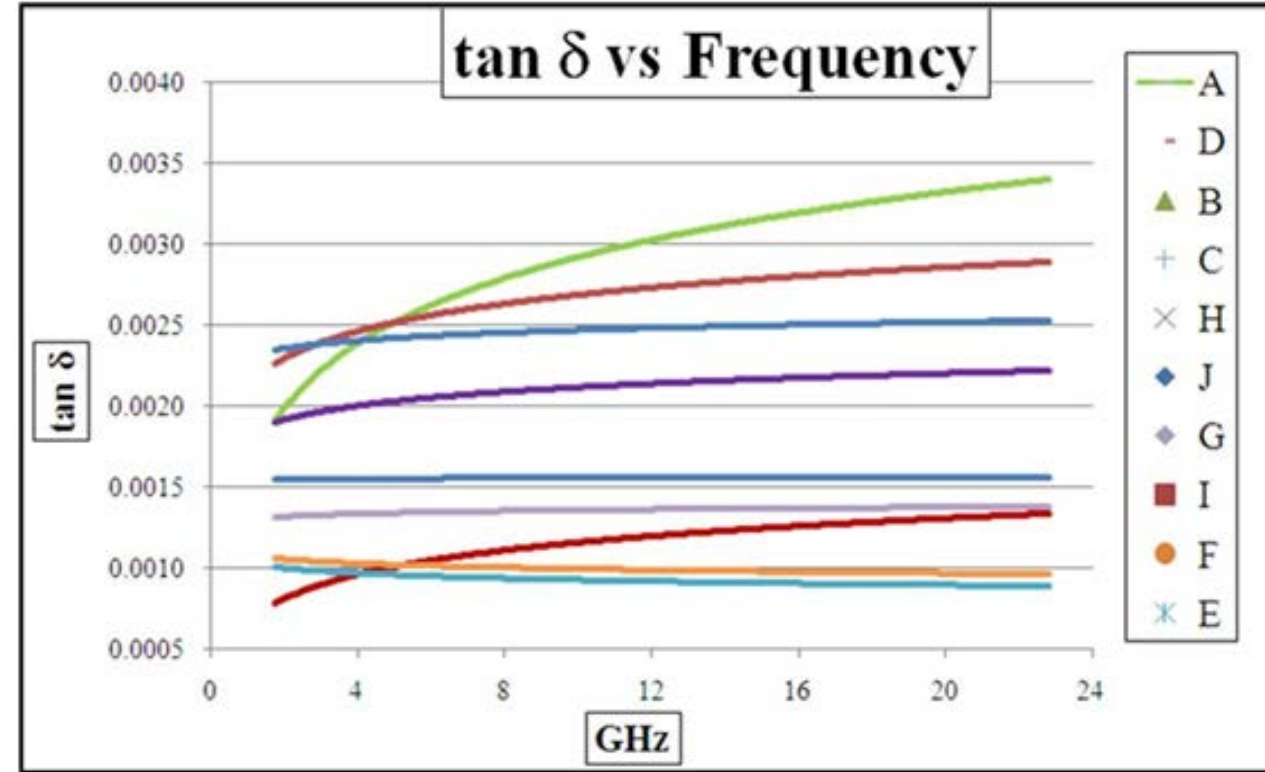
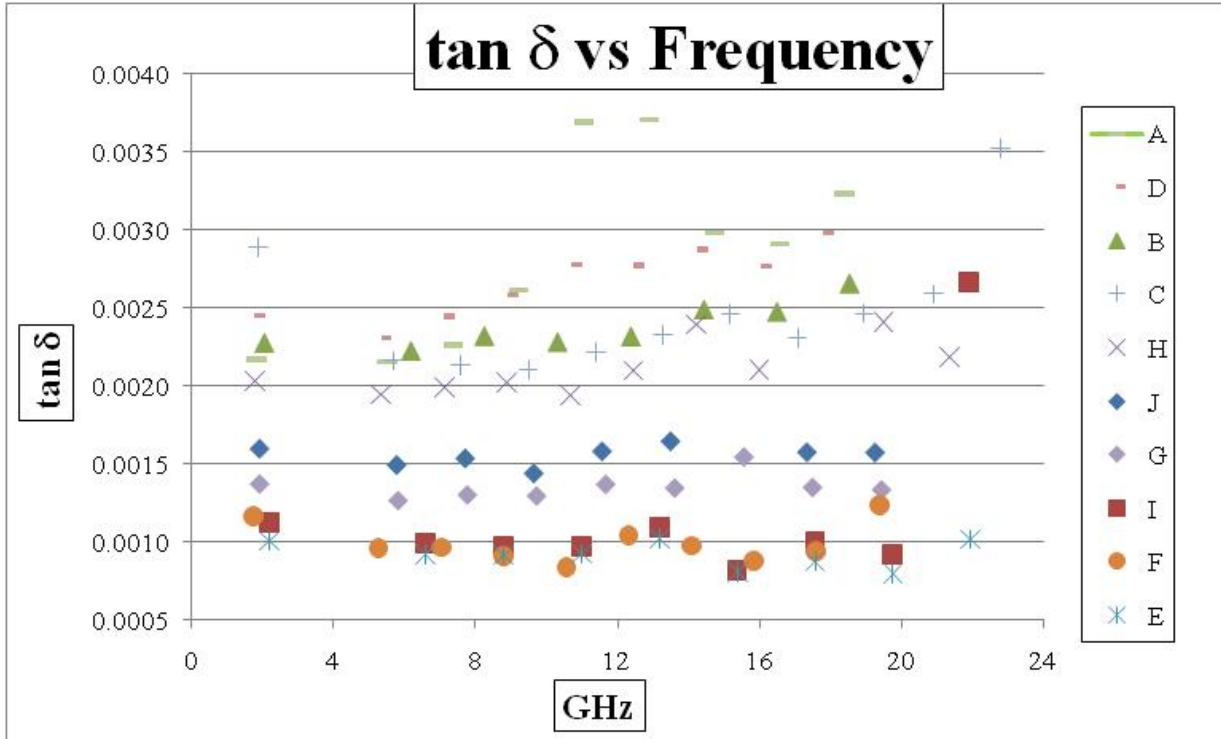
Bereskin E_r vs Frequency



Sample Name	Nominal DT [mils]	Expected E_r @ 10 GHz	Expected $\tan \delta$ @ 10 GHz	Bereskin DK	Bereskin Loss	Frequency Range [GHz]
A	6	3.4	0.0040	3.08	0.0029	1.84 - 18.42
B	4	2.5	0.0020	2.46	0.0024	2.06 - 18.54
C	4	3	0.0016	2.90	0.0024	1.90 - 22.81
D	5	3.5	0.0028	3.28	0.0027	1.79 - 19.58
E	5	2.2	0.0009	2.17	0.0009	2.20 - 21.96
F	5	3.5	0.0015	3.36	0.0010	1.76 - 19.40
G	5	2.94	0.0012	2.76	0.0014	1.95 - 19.45
H	5	3.5	0.0020	3.32	0.0021	1.77 - 21.35
I	5	2.2	0.0009	2.17	0.0010	2.20 - 21.89
J	5	3	0.0011	2.81	0.0016	1.93 - 19.26

[Wynants]

Bereskin Clamped Stripline Resonator Data



[Wynants]

Analysis and Conclusions

- **Thickness**
- **Basic Z Coupon Data**
- **Normal Dk Data Comparison at 10 GHz**
- **Df Data Comparison at 10 GHz**
- **Normal Dk and Df Data Comparison Above 10 GHz**
- **In-Plane Dk Comparison at 10 GHz and Beyond**
- **Discussion of Conclusions**

Thickness

- Thickness measurements agree fairly well with nominal
- For thin layers, thickness measurement bias is the largest source of error

Sample	Nominal Expected (um)	Oliver Micrometer	DeGroot Micrometer	Nwachukwu Micrometer	Wynants Micrometer	Oliver X-Section
A	150	150	144	132*	147	148
B	100	98	97	99	99	96
C	100	100	101	100	102	99
D	125	132	130	130	130	131
E	125	123	124	119	124	121
F	125	133	134	124	135	130
G	125	126	130	119	127	125
H	125	127	130	127	132	127
I	125	128	130	126	132	126
J	125	124	132	127	135	124

*Sent a 125 um clad by accident

Normal Dk Analysis up to 10 GHz

- **Extract from TDR coupons**

- Lots more variables = lots more variation.
- Low frequency <2 GHz (200 ps pulse)

LOW Frequency (<2 GHz)		
Sample	Expected Normal Dk @ 10 GHz	Extraction from TDR Zo
A	3.3	3.0
B	2.5	2.1
C	3	2.9
D	3.5	3.0
E	2.2	1.8
F	3.6	3.4
G	2.94	2.2
H	3.5	3.1
I	2.2	1.8
J	3	2.7

- **Normal permittivity analysis using three different methods**

- Good agreement. Better than expected.

Sample	Normal Permittivity at 10 GHz			
	Expected Normal Dk @ 10 GHz	Microstrip Group Delay (Oliver)	Differential Phase Length (Coonrod)	Bereskin Resonator (Wynants)
A	3.3	3.25	3.27	3.08
B	2.5	2.46	2.53	2.46
C	3	2.96	3.12	2.9
D	3.5	3.43	3.51	3.28
E	2.2	2.2	2.22	2.17
F	3.6	3.74	3.67	3.36
G	2.94	2.83	2.94	2.76
H	3.5	3.45	3.58	3.32
I	2.2	2.22	2.25	2.17
J	3	2.98	3.05	2.81

Df at 10 GHz – Cavity Resonators and Bereskin

- **Better agreement than expected around 10 GHz.**

Sample	Datasheet Df @ 10 GHz	Split Cylinder (DeGroot)		Split Post Dielectric Res. (Coonrod)	Rectangular Resonator (Oliver)	Bereskin Stripline (Wynants)
		Single	Stack of 2			
A	0.0040	0.00112	0.00176	0.0017	0.0025	0.0032
B	0.0020	0.00181	0.00241	0.0016	0.0033	0.0023
C	0.0016	0.00173	0.00177	0.0018	0.0013	0.0021
D	0.0028	0.00201	0.00200	0.0025	0.0021	0.0026
E	0.0009	0.00071	0.00075	0.0007	0.0008	0.0009
F	0.0015	0.00051	0.00051	0.0008	0.0008	0.0008
G	0.0012	0.00120	0.00122	0.0011	0.0014	0.0013
H	0.0020	0.00200	0.00201	0.0023	0.0027	0.0019
I	0.0009	0.00128	0.00132	0.0014	0.0021	0.0009
J	0.0011	0.00128	0.00131	0.0017	0.0012	0.0014

Df Resonator Measurements Beyond 10 GHz

- **Promising result for higher frequency characterization.**

Sample	Split Post (Coonrod)	Bereskin Stripline (Wynants)	Open Resonator (Oliver)			
	20 GHz	20 GHz	26 GHz	40 GHz	49 GHz	60 GHz
A	0.0027	0.0033	0.0022	0.0023	0.0029	0.0028
B	0.0020	0.0027	0.0045	0.0048	0.0050	0.0038
C	0.0025	0.0024	0.0021	0.0024	0.0023	0.0020
D	0.0041	0.0030	0.0032	0.0036	0.0035	0.0031
E	0.0015	0.0008	0.0009	0.0014	0.0011	0.0008
F	0.0020	0.0012	0.0008	0.0011	0.0009	0.0015
G	0.0024	0.0024	0.0016	0.0018	0.0019	0.0014
H	0.0038	0.0019	0.0029	0.0032	0.0037	0.0022
I	0.0019	0.0009	0.0016	0.0023	0.0021	0.0023
J	0.0024	0.0016	0.0021	0.0023	0.0025	0.0021

Normal Dk Beyond 10 GHz

- Promising result for higher frequency characterization.

Sample	uStrip Group Delay (Oliver)			Differential Phase Length (Coonrod)				Bereskin (Wynants)	
	10 GHz	26 GHz	40 GHz	10 GHz	26 GHz	40 GHz	100 GHz	10 GHz	26 GHz
A	3.25	3.30	3.37	3.27	3.26	3.25	3.22	3.46	3.42
B	2.46	2.48	2.49	2.53	2.51	2.51	2.50	2.87	2.80
C	2.96	2.97	3.02	3.12	3.09	3.08	3.07	3.39	3.39
D	3.43	3.49	3.63	3.51	3.49	3.49	3.49	3.43	3.46
E	2.20	2.23	2.25	2.22	2.21	2.21	2.20	2.29	2.25
F	3.74	3.78	3.94	3.67	3.63	3.64	3.66	3.72	3.61
G	2.83	2.89	2.98	2.94	2.93	2.92	2.91	2.89	2.93
H	3.45	3.52	3.57	3.58	3.56	3.54	3.52	3.53	3.53
I	2.22	2.24	2.25	2.25	2.24	2.24	2.23	2.34	2.37
J	2.98	3.01	3.03	3.05	3.04	3.03	3.02	2.95	2.94

In-Plane Dk 10 GHz and Beyond

- It is important to understand that In-Plane Dk and Normal Dk measurements do not always agree.

Sample	Split Post (Coonrod)		Split Cylinder (DeGroot)		Rect. Resonator (Oliver)	Open Resonator (Oliver)				Quasi-Optical Free Space (Nwachukwu)
	10 GHz	20 GHz	Single Sheet	Two Sheets	10 GHz	26 GHz	40 GHz	49 GHz	60 GHz	40-60 GHz
A	3.448	3.440	3.540	3.545	3.46	3.42	3.41	3.41	3.41	3.9*
B	2.789	2.787	2.878	2.830	2.87	2.80	2.80	2.79	2.78	2.0
C	3.317	3.308	3.420	3.379	3.39	3.39	3.39	3.38	3.38	3.2
D	3.445	3.436	3.511	3.500	3.43	3.46	3.45	3.44	3.42	3.25
E	2.26	2.254	2.276	2.254	2.29	2.25	2.24	2.23	2.21	2.35
F	3.577	3.568	3.675	3.648	3.72	3.61	3.59	3.56	3.52	3.8
G	2.991	2.893	2.927	2.904	2.89	2.93	2.91	2.89	2.87	3.1
H	3.424	3.402	3.513	3.477	3.53	3.53	3.53	3.52	3.51	3.7
I	2.297	2.281	2.363	2.342	2.34	2.37	2.36	2.36	2.36	2.5
J	2.894	2.883	2.911	2.892	2.95	2.94	2.93	2.93	2.92	3.15

Conclusions...Take-Aways

- **“Tribal Knowledge” over the years has propagated the message that high frequency test methods are “All Over the Place”...This study does not support this argument.**
- **Accurate and precise thickness measurement is critical for 10 GHz and beyond.**
- **Normal Dk agree well between transmission line methods and stripline resonator methods.**
- **Dk is different when measured normal to the plane (Tx Lines) and in-plane (Resonators)**
- **Df is about the same in both directions (Resonator versus Stripline)**
- **Transmission line methods extracting phase are most promising for future method development for Normal Dk.**
- **Resonator methods are the most useful method for measuring Df at high frequencies.**

Acknowledgements

The following companies contributed samples material and/or test support for support this work:

- **DuPont Electronics and Communications**
- **Rogers Corporation**
 - **Both Rogers Advanced Connectivity Solutions and Arlon represented**
- **Taconic Advanced Dielectrics Division**
- **Connected Community Networks**
- **ISOLA**
- **Park Electrochemical Corporation**
- **Panasonic Electronic Materials – Thank You Tony Senese**
- **Sean Sweeny, a student at SUNY-Binghamton performed testing as a Summer Intern at DuPont**

References

- 1. <http://cp.literature.agilent.com/litweb/pdf/5989-5384EN.pdf>

Thank you!

QUESTIONS?